

# International Journal of Physical Sciences

Volume 8 Number 26 16 July, 2013

ISSN 1992 - 1950



*Academic  
Journals*

## ABOUT IJPS

The **International Journal of Physical Sciences (IJPS)** is published weekly (one volume per year) by Academic Journals.

**International Journal of Physical Sciences (IJPS)** is an open access journal that publishes high-quality solicited and unsolicited articles, in English, in all Physics and chemistry including artificial intelligence, neural processing, nuclear and particle physics, geophysics, physics in medicine and biology, plasma physics, semiconductor science and technology, wireless and optical communications, materials science, energy and fuels, environmental science and technology, combinatorial chemistry, natural products, molecular therapeutics, geochemistry, cement and concrete research, metallurgy, crystallography and computer-aided materials design. All articles published in IJPS are peer-reviewed.

## Submission of Manuscript

Submit manuscripts as e-mail attachment to the Editorial Office at: [ijps@academicjournals.org](mailto:ijps@academicjournals.org), [ijps.acadjourn@gmail.com](mailto:ijps.acadjourn@gmail.com). A manuscript number will be mailed to the corresponding author shortly after submission.

For all other correspondence that cannot be sent by e-mail, please contact the editorial office (at [ijps@academicjournals.org](mailto:ijps@academicjournals.org)).

The International Journal of Physical Sciences will only accept manuscripts submitted as e-mail attachments.

Please read the **Instructions for Authors** before submitting your manuscript. The manuscript files should be given the last name of the first author.

## Editors

### **Prof. Sanjay Misra**

*Department of Computer Engineering, School of Information and Communication Technology  
Federal University of Technology, Minna,  
Nigeria.*

### **Prof. Jr-Hau He**

*National Taiwan University  
Roosevelt, MD-518,  
Taipei 106,  
Taiwan*

### **Dr. G. Suresh Kumar**

*Senior Scientist and Head Biophysical Chemistry  
Division Indian Institute of Chemical Biology  
(IICB)(CSIR, Govt. of India),  
Kolkata 700 032,  
INDIA.*

### **Dr. Remi Adewumi Oluyinka**

*Senior Lecturer,  
School of Computer Science  
Westville Campus  
University of KwaZulu-Natal  
Private Bag X54001  
Durban 4000  
South Africa.*

### **Prof. Hyo Choi**

*Graduate School  
Gangneung-Wonju National University  
Gangneung,  
Gangwondo 210-702, Korea*

### **Prof. Kui Yu Zhang**

*Laboratoire de Microscopies et d'Etude de  
Nanostructures (LMEN)  
Département de Physique, Université de Reims,  
B.P. 1039. 51687,  
Reims cedex,  
France.*

### **Prof. R. Vittal**

*Research Professor,  
Department of Chemistry and Molecular  
Engineering  
Korea University, Seoul 136-701,  
Korea.*

### **Prof Mohamed Bououdina**

*Director of the Nanotechnology Centre  
University of Bahrain  
PO Box 32038,  
Kingdom of Bahrain*

### **Prof. Geoffrey Mitchell**

*School of Mathematics,  
Meteorology and Physics  
Centre for Advanced Microscopy  
University of Reading Whiteknights,  
Reading RG6 6AF  
United Kingdom.*

### **Dr. Duduku Krishnaiah**

*Chemical Engineering Programme  
School of Engineering and Information Technology  
Universiti Malaysia Sabah, 88999  
Kota Kinabalu  
Sabah,  
Malaysia.*

### **Dr. Sushil Kumar**

*Geophysics Group,  
Wadia Institute of Himalayan Geology,  
P.B. No. 74 Dehra Dun - 248001(UC)  
India.*

### **Prof. Suleyman KORKUT**

*Duzce University  
Faculty of Forestry  
Department of Forest Industrial Engineering  
Beciyorukler Campus 81620  
Duzce-Turkey*

### **Prof. Nazmul Islam**

*Department of Basic Sciences &  
Humanities/Chemistry,  
Techno Global-Balurghat, Mangalpur, Near District  
Jail P.O: Beltalpark, P.S: Balurghat, Dist.: South  
Dinajpur,  
Pin: 733103,India.*

### **Prof. Dr. Ismail Musirin**

*Centre for Electrical Power Engineering Studies  
(CEPES), Faculty of Electrical Engineering, Universiti  
Teknologi Mara,  
40450 Shah Alam,  
Selangor, Malaysia*

### **Prof. Mohamed A. Amr**

*Nuclear Physic Department, Atomic Energy Authority  
Cairo 13759,  
Egypt.*

### **Dr. Armin Shams**

*Artificial Intelligence Group,  
Computer Science Department,  
The University of Manchester.*

## Editorial Board

**Prof. Salah M. El-Sayed**

*Mathematics. Department of Scientific Computing,  
Faculty of Computers and Informatics,  
Benha University. Benha ,  
Egypt.*

**Dr. Rowdra Ghatak**

*Associate Professor  
Electronics and Communication Engineering Dept.,  
National Institute of Technology Durgapur  
Durgapur West Bengal*

**Prof. Fong-Gong Wu**

*College of Planning and Design, National Cheng Kung  
University  
Taiwan*

**Dr. Abha Mishra.**

*Senior Research Specialist & Affiliated Faculty.  
Thailand*

**Dr. Madad Khan**

*Head  
Department of Mathematics  
COMSATS University of Science and Technology  
Abbottabad, Pakistan*

**Prof. Yuan-Shyi Peter Chiu**

*Department of Industrial Engineering & Management  
Chaoyang University of Technology  
Taichung, Taiwan*

**Dr. M. R. Pahlavani,**

*Head, Department of Nuclear physics,  
Mazandaran University,  
Babolsar-Iran*

**Dr. Subir Das,**

*Department of Applied Mathematics,  
Institute of Technology, Banaras Hindu University,  
Varanasi*

**Dr. Anna Oleksy**

*Department of Chemistry  
University of Gothenburg  
Gothenburg,  
Sweden*

**Prof. Gin-Rong Liu,**

*Center for Space and Remote Sensing Research  
National Central University, Chung-Li,  
Taiwan 32001*

**Prof. Mohammed H. T. Qari**

*Department of Structural geology and remote sensing  
Faculty of Earth Sciences  
King Abdulaziz UniversityJeddah,  
Saudi Arabia*

**Dr. Jyhwen Wang,**

*Department of Engineering Technology and Industrial  
Distribution  
Department of Mechanical Engineering  
Texas A&M University  
College Station,*

**Prof. N. V. Sastry**

*Department of Chemistry  
Sardar Patel University  
Vallabh Vidyanagar  
Gujarat, India*

**Dr. Edilson Ferneda**

*Graduate Program on Knowledge Management and IT,  
Catholic University of Brasilia,  
Brazil*

**Dr. F. H. Chang**

*Department of Leisure, Recreation and Tourism  
Management,  
Tzu Hui Institute of Technology, Pingtung 926,  
Taiwan (R.O.C.)*

**Prof. Annapurna P.Patil,**

*Department of Computer Science and Engineering,  
M.S. Ramaiah Institute of Technology, Bangalore-54,  
India.*

**Dr. Ricardo Martinho**

*Department of Informatics Engineering, School of  
Technology and Management, Polytechnic Institute of  
Leiria, Rua General Norton de Matos, Apartado 4133, 2411-  
901 Leiria,  
Portugal.*

**Dr Driss Miloud**

*University of mascara / Algeria  
Laboratory of Sciences and Technology of Water  
Faculty of Sciences and the Technology  
Department of Science and Technology  
Algeria*

# Instructions for Author

**Electronic submission** of manuscripts is strongly encouraged, provided that the text, tables, and figures are included in a single Microsoft Word file (preferably in Arial font).

The **cover letter** should include the corresponding author's full address and telephone/fax numbers and should be in an e-mail message sent to the Editor, with the file, whose name should begin with the first author's surname, as an attachment.

## Article Types

Three types of manuscripts may be submitted:

**Regular articles:** These should describe new and carefully confirmed findings, and experimental procedures should be given in sufficient detail for others to verify the work. The length of a full paper should be the minimum required to describe and interpret the work clearly.

**Short Communications:** A Short Communication is suitable for recording the results of complete small investigations or giving details of new models or hypotheses, innovative methods, techniques or apparatus. The style of main sections need not conform to that of full-length papers. Short communications are 2 to 4 printed pages (about 6 to 12 manuscript pages) in length.

**Reviews:** Submissions of reviews and perspectives covering topics of current interest are welcome and encouraged. Reviews should be concise and no longer than 4-6 printed pages (about 12 to 18 manuscript pages). Reviews are also peer-reviewed.

## Review Process

All manuscripts are reviewed by an editor and members of the Editorial Board or qualified outside reviewers. Authors cannot nominate reviewers. Only reviewers randomly selected from our database with specialization in the subject area will be contacted to evaluate the manuscripts. The process will be blind review.

Decisions will be made as rapidly as possible, and the journal strives to return reviewers' comments to authors as fast as possible. The editorial board will re-review manuscripts that are accepted pending revision. It is the goal of the IJPS to publish manuscripts within weeks after submission.

## Regular articles

All portions of the manuscript must be typed double-spaced and all pages numbered starting from the title page.

**The Title** should be a brief phrase describing the contents of the paper. The Title Page should include the authors' full names and affiliations, the name of the corresponding author along with phone, fax and E-mail information. Present addresses of authors should appear as a footnote.

**The Abstract** should be informative and completely self-explanatory, briefly present the topic, state the scope of the experiments, indicate significant data, and point out major findings and conclusions. The Abstract should be 100 to 200 words in length. Complete sentences, active verbs, and the third person should be used, and the abstract should be written in the past tense. Standard nomenclature should be used and abbreviations should be avoided. No literature should be cited.

Following the abstract, about 3 to 10 key words that will provide indexing references should be listed.

A list of non-standard **Abbreviations** should be added. In general, non-standard abbreviations should be used only when the full term is very long and used often. Each abbreviation should be spelled out and introduced in parentheses the first time it is used in the text. Only recommended SI units should be used. Authors should use the solidus presentation (mg/ml). Standard abbreviations (such as ATP and DNA) need not be defined.

**The Introduction** should provide a clear statement of the problem, the relevant literature on the subject, and the proposed approach or solution. It should be understandable to colleagues from a broad range of scientific disciplines.

**Materials and methods** should be complete enough to allow experiments to be reproduced. However, only truly new procedures should be described in detail; previously published procedures should be cited, and important modifications of published procedures should be mentioned briefly. Capitalize trade names and include the manufacturer's name and address. Subheadings should be used. Methods in general use need not be described in detail.

**Results** should be presented with clarity and precision.

The results should be written in the past tense when describing findings in the authors' experiments. Previously published findings should be written in the present tense. Results should be explained, but largely without referring to the literature. Discussion, speculation and detailed interpretation of data should not be included in the Results but should be put into the Discussion section.

**The Discussion** should interpret the findings in view of the results obtained in this and in past studies on this topic. State the conclusions in a few sentences at the end of the paper. The Results and Discussion sections can include subheadings, and when appropriate, both sections can be combined.

**The Acknowledgments** of people, grants, funds, etc should be brief.

**Tables** should be kept to a minimum and be designed to be as simple as possible. Tables are to be typed double-spaced throughout, including headings and footnotes. Each table should be on a separate page, numbered consecutively in Arabic numerals and supplied with a heading and a legend. Tables should be self-explanatory without reference to the text. The details of the methods used in the experiments should preferably be described in the legend instead of in the text. The same data should not be presented in both table and graph form or repeated in the text.

**Figure legends** should be typed in numerical order on a separate sheet. Graphics should be prepared using applications capable of generating high resolution GIF, TIFF, JPEG or Powerpoint before pasting in the Microsoft Word manuscript file. Tables should be prepared in Microsoft Word. Use Arabic numerals to designate figures and upper case letters for their parts (Figure 1). Begin each legend with a title and include sufficient description so that the figure is understandable without reading the text of the manuscript. Information given in legends should not be repeated in the text.

**References:** In the text, a reference identified by means of an author's name should be followed by the date of the reference in parentheses. When there are more than two authors, only the first author's name should be mentioned, followed by 'et al'. In the event that an author cited has had two or more works published during the same year, the reference, both in the text and in the reference list, should be identified by a lower case letter like 'a' and 'b' after the date to distinguish the works.

Examples:

Abayomi (2000), Agindotan et al. (2003), (Kelebeni, 1983), (Usman and Smith, 1992), (Chege, 1998;

1987a,b; Tijani, 1993,1995), (Kumasi et al., 2001)

References should be listed at the end of the paper in alphabetical order. Articles in preparation or articles submitted for publication, unpublished observations, personal communications, etc. should not be included in the reference list but should only be mentioned in the article text (e.g., A. Kingori, University of Nairobi, Kenya, personal communication). Journal names are abbreviated according to Chemical Abstracts. Authors are fully responsible for the accuracy of the references.

Examples:

Ogunseitan OA (1998). Protein method for investigating mercuric reductase gene expression in aquatic environments. *Appl. Environ. Microbiol.* 64:695-702.

Gueye M, Ndoye I, Dianda M, Danso SKA, Dreyfus B (1997). Active N<sub>2</sub> fixation in several *Faidherbia albida* provenances. *Ar. Soil Res. Rehabil.* 11:63-70.

Charnley AK (1992). Mechanisms of fungal pathogenesis in insects with particular reference to locusts. In: Lomer CJ, Prior C (eds) *Biological Controls of Locusts and Grasshoppers: Proceedings of an international workshop held at Cotonou, Benin.* Oxford: CAB International, pp 181-190.

Mundree SG, Farrant JM (2000). Some physiological and molecular insights into the mechanisms of desiccation tolerance in the resurrection plant *Xerophyta viscasa* Baker. In Cherry et al. (eds) *Plant tolerance to abiotic stresses in Agriculture: Role of Genetic Engineering*, Kluwer Academic Publishers, Netherlands, pp 201-222.

### Short Communications

Short Communications are limited to a maximum of two figures and one table. They should present a complete study that is more limited in scope than is found in full-length papers. The items of manuscript preparation listed above apply to Short Communications with the following differences: (1) Abstracts are limited to 100 words; (2) instead of a separate Materials and Methods section, experimental procedures may be incorporated into Figure Legends and Table footnotes; (3) Results and Discussion should be combined into a single section.

**Proofs and Reprints:** Electronic proofs will be sent (e-mail attachment) to the corresponding author as a PDF file. Page proofs are considered to be the final version of the manuscript. With the exception of typographical or minor clerical errors, no changes will be made in the manuscript at the proof stage.

**Copyright: © 2013, Academic Journals.**

All rights Reserved. In accessing this journal, you agree that you will access the contents for your own personal use but not for any commercial use. Any use and or copies of this Journal in whole or in part must include the customary bibliographic citation, including author attribution, date and article title.

Submission of a manuscript implies: that the work described has not been published before (except in the form of an abstract or as part of a published lecture, or thesis) that it is not under consideration for publication elsewhere; that if and when the manuscript is accepted for publication, the authors agree to automatic transfer of the copyright to the publisher.

**Disclaimer of Warranties**

In no event shall Academic Journals be liable for any special, incidental, indirect, or consequential damages of any kind arising out of or in connection with the use of the articles or other material derived from the IJPS, whether or not advised of the possibility of damage, and on any theory of liability.

This publication is provided "as is" without warranty of any kind, either expressed or implied, including, but not limited to, the implied warranties of merchantability, fitness for a particular purpose, or non-infringement. Descriptions of, or references to, products or publications does not imply endorsement of that product or publication. While every effort is made by Academic Journals to see that no inaccurate or misleading data, opinion or statements appear in this publication, they wish to make it clear that the data and opinions appearing in the articles and advertisements herein are the responsibility of the contributor or advertiser concerned. Academic Journals makes no warranty of any kind, either express or implied, regarding the quality, accuracy, availability, or validity of the data or information in this publication or of any other publication to which it may be linked.

## ARTICLES

### CHEMISTRY

**Synthesis, characterization and neuropharmacological activity of novel angular pentacyclic phenothiazine** 1374

Odin E. M., Onoja P. K. and Saleh J. F

**Quantum chemical calculations on molecular structures and solvents effect on 4-nitropicolinic and 4-methoxypicolinic acid** 1382

Semire Banjo and Adeoye Idowu Olatunbosun

### COMPUTER SCIENCE

**Neuro-fuzzy decision learning on supply chain configuration** 1393

J. C. Garcia Infante, J. J. Medel Juarez and J. C. Sanchez Garcia

### COMMUNICATION TECHNOLOGY

**Simulation and analysis: The effect of mobility on IPTV (VOD) over wi-max using OPNET** 1401

Gurmeet Singh and Amit Grover

Full Length Research Paper

# Synthesis, characterization and neuropharmacological activity of novel angular pentacyclic phenothiazine

Odin E. M.\*, Onoja P. K. and Saleh J. F.

Department of Pure and Industrial Chemistry, Kogi State University, Anyigba, Nigeria.

Accepted 08 July, 2013

13H-5,14-dihydroquinoxalino[2,3-a]phenothiazine (a new pentacyclic ring system) was synthesized by condensation of diphenylamine and sulphur, which on nitration yielded 1-nitrophenothiazine. Reduction of this compound afforded 1-aminophenothiazine dihydrochloride and subsequent protection of this product with acetic anhydride gave 1-acetylaminophenothiazine. The nitration of this acetylated compound yielded two isomeric compounds: 1-amino-2-nitrophenothiazine and 1-amino-4-nitrophenothiazine. The reduction of the ortho isomer furnished 1,2-diaminophenothiazine which when added to catechol and refluxed with ethanol gave the pentacyclic product 13H-5,14-dihydroquinoxalino[2,3-a]phenothiazine. Structures were established by analytical and spectral data. The results of the neuropharmacological screening data revealed that the novel system possessed neurosedative properties. The ability of this compound to antagonise fortwin – induced climbing behaviour in mice was correlated with neuroleptic potential.

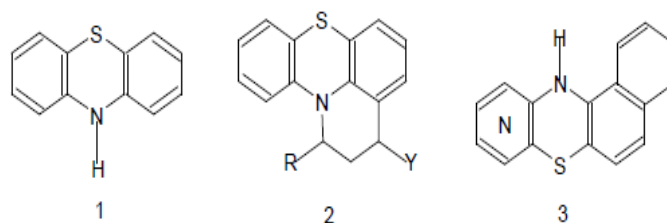
**Key words:** 13H-5,14-dihydroquinoxalino[2,3-a]phenothiazine, pentacyclic, phenothiazine, neurosedative, fortwin-induced.

## INTRODUCTION

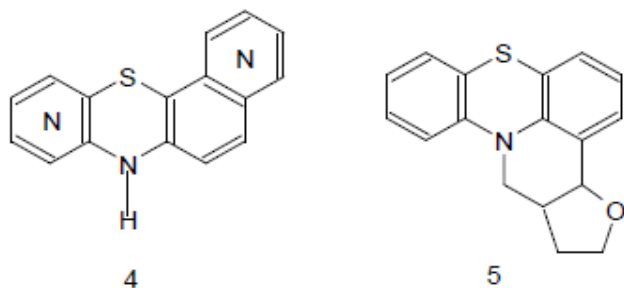
The chemistry of phenothiazines has generated intensive scientific interest due to their biological properties (Ujuwala et al., 2012). Great work has been done on the bioactivity of phenothiazine and its derivatives. Phenothiazine itself is found to be a worming agent for livestock. The pesticidal action of phenothiazine results from the fact that they affect the nervous system of insects by inhibiting the breakdown of acetylcholine. The derivatives of phenothiazine have been studied for their antipsychotic properties (Luiza et al., 2007; Whitaker, 2004). They constitute the largest of the five classes of antipsychotic drugs. The antipsychotic activities of phenothiazine have been attributed to the basic nitrogen of the thiazine ring which donates electrons to the biological receptors by a charge transfer mechanism and also the ability of substituting the hydrogen atom to the nitrogen atom by substituent groups which further

enhances the pharmacological property (Abdel-Monem and Portoghese, 1972; Martina et al., 2007).

The chemistry of the linear phenothiazine (1) is well developed (Abdel-Rahman et al., 2013; Okafor 1971; 1978). The non-linear aza phenothiazine is relatively understudied in spite of their pharmacological importance in medicine, agriculture and industry (Ezema et al., 2012; Okoro et al., 2009).



While tetracyclic, N-(2,3-dihydro-1H-pyrido[3,2,1-kl]phenothiazines) of type **2** have previously been reported (Alan et al., 1999; Tim et al., 2012), very few of the non linear tetracyclic phenothiazine of type **3** benzo[a]azaphenothiazine and its diaza-analogue type **4** have been reported (Chuan et al., 2012; Okoro et al., 2009).



Still grossly understudied are the non-linear (angular) pentacyclic phenothiazine systems in spite of their known pharmaceutical and industrial applications. Pentacyclic phenothiazines of type **5** (Tetrahydro-3aH-furo[2,3:4,5]pyrido[3,2,1-kl]phenothiazine) have previously been prepared by the treatment of 10-[benzotriazol-1-yl] methyl phenothiazine with cyclic hydrofuran and 3,4-2H-dihydropyran (Abdel-Rahman et al., 2013; Alan et al., 1999). The non-linear pentacyclic aza phenothiazine of type **13** to the best of our knowledge has not been reported. In this paper we report the synthesis of the pentacyclic phenothiazine **13** (a new pentacyclic ring system) and its pharmacological properties.

## MATERIALS AND METHODS

All chemicals were obtained from different sources (Lavans, Aldrich, Merck) and were used without further purification. The melting points were determined on a SMP3 melting point apparatus and are reported in degree Celsius uncorrected. Column chromatography was performed in Scharlan silica gel 60 (70 – 230 mesh).  $^1\text{H}$  and  $^{13}\text{C}$  –NMR spectra were recorded on a Varian Gemini 2000 spectrophotometer operating 200 and 50 MHz respectively. Chemical shifts were recorded as  $\delta$  values in ppm referenced to the solvent. HPLC separations were performed in a Bulk Scientific 500 apparatus using a reverse phase Lichrospher 100RP-18(5  $\mu\text{m}$ ) column at room temperature (eluent: methanol/water-8:2, v/v). The Infrared (IR) spectra were recorded in  $\text{cm}^{-1}$  on a Bulk Scientific 500 Spectrophotometer. The mass spectra were recorded on a Shimadzu GCMS-QP-1000E, mass spectrometer at 70 eV and elementary analysis for C, H, S and N on a Perkin-Elmer analyzer 2400.

## Drugs

Diazepam and Nitrazepam were obtained from Roche Nigeria Ltd, while pentobarbital and apomorphine were obtained from Sigma Chemical Company, USA. All drugs were freshly prepared. Parallel control experiments were done in each case to correct possible effects caused by the vehicle alone.

## Animals

All experiments performed on laboratory animals in this study followed the "Principle of laboratory animal care" (NIH publication No 85-23, revised 1985). Swiss albino mice (20 to 30 g) and wistar rats (180 to 200 g) of either sex were used. All the animals were maintained at the Animal Facility Centre of Kogi State University at standard conditions and temperature (25°C) and fed with standard diet (Ladokum feeds, Ibadan and water *ad libitum*).

## Synthesis

The synthetic routes for all compounds are outlined in the scheme 1 and the details are given below:

### Phenothiazine (1)

A mixture of the corresponding diphenylamine (13 g, 3.0 mol) and sulphur (1.2 g, 0.834 mol) was heated in a glycerol oil bath to 195°C. After cooling to 100°C, elemental iodine was added while heating continued. The separation of hydrogen sulphide was observed at 170°C and was decomposed by leading in 5% aqueous sodium hydroxide solution. The mixture was heated to 185°C and held at this temperature for 45 min. The bath was cooled to 50°C and was diluted with benzene (100 ml). This was filtered hot in a vacuum pump to remove the excess sulphur. The yellowish filtrate was concentrated using a rotary evaporator. The product was dried and purified by column chromatography. Yield 11.06 g (80.5%), m.p. 184-186°C. IR ( $\text{Vmax/cm}^{-1}$ ): 2999 (NH), 2859-2861 (C-H arom.), 717(C-H bending), 1197-1211 (C-H in-plane) and 1300-1411 (C-N arom.). UV: 311 (log  $\epsilon$  3.3281)nm.  $^1\text{H}$  NMR (200 MHz, DMSO): 7.32 (d, 2H), 7.34 (d, 4H), 7.29 (s, 6H), 7.28 (s, 8H), 7.04 (s, 3H), 7.06 (s, 7H), 6.99-6.92 (m, 1H), 6.98-6.91 (m, 9H), 11.48 (s, -NH proton).  $^{13}\text{C}$  NMR (50MHz, DMSO): 140.7 (C. Arom. Ring), 120.8 (CNH), 110.2, 113.3, 121.4, 122.6, 125.2, 139.6, 103.2, 118.9, 124.9, 130.6 (CH and C). Anal. Cal. For  $\text{C}_{12}\text{H}_9\text{NS}$ : C, 72.40; H, 6.30; N, 9.72; S, 22.22%. Found: C, 72.29; H, 6.34; N, 9.69; S, 22.14%.

### 1-Nitrophenothiazine (7)

Concentrated nitric acid (10 ml, 0.5 mol) was placed in a 200 ml round bottom flask, while concentrated sulphuric acid (10 ml, 0.5 mol) was added to it portion wise over 30 min. With efficient stirring at room temperature, compound **1**(15 g, mol) was added. The mixture was refluxed in a water bath while the temperature was held at 50°C for 40 min. The product was washed with 500 ml cold water and filtered with suction on a Buchner funnel, dried and purified by column chromatography. Yield 20.40 g (95%), m.p. 160-161°C, IR: 2910 (C-H stretch), 972 (C-H bend), 1611-1462 (Arom. Skeleton), 1580-1550 and 1345-1332 (aromatic nitro gr. Vibrations),UV: 320 nm.  $^1\text{H}$  NMR: 7.21 (d,1H), 6.95 (d,2H), 6.91 (s,6H), 6.80 (m, 7H), 6.92 (d,8H), 8.82 (d, 9H), 10.30-9.82 (s, NH protons).  $^{13}\text{C}$  NMR: 141.8 (C arom. Ring), 121.9 (CNH), 130.8 ( $\text{NO}_2$ ), 111.5, 112.4, 121.5, 123.2, 126.7, 140.1, 115.1, 117.3, 122.8, 123.4 (CH and C). Anal. Cal. For  $\text{C}_{12}\text{H}_8\text{N}_2\text{S}$ : C, 67.89; H, 3.80; N, 13.20; S, 15.11%. Found: C, 67.83; H, 3.78; N, 13.18; S, 15.09%.

### 1-Aminophenothiazine dihydrochloride (8)

Iron powder (20 g, 0.36 mol) was added portionwise to 1-nitrophenothiazine (17 g, 0.07 mol) suspended in 100 ml warm water containing 5 ml concentrated hydrochloric acid. The mixture was heated to 60°C and held at this temperature for 1½ h. The

reaction mixture was filtered hot and the filtrate treated with excess concentrated hydrochloric acid, dried and purified by column chromatography (silica gel, DMSO). Yield: 13.50 g (79.4%); m.p. 151-158°C. IR: 3541 (N-H stretch), 2819-2821 (C-H stretch), 1093 (C-H inplane), 1320 (C-N stretch), 1684-1698 (Arom. skeletal system). UV 312 nm. <sup>1</sup>H NMR: 1.15-1.31 (m, 9H), 3.02-3.21 (m, 3H), 4.14-4.50 (m, 2H), 7.00-7.32(m, 8H), 10.30 (br. s, 7H), 1.17-1.33 ( m, 5H), 3.16-3.39 ( m, 1H), 3.57(m, 3H), 4.17-4.44 ( m,10H) 9.76 (s, NH protons), 5.70 (m,NH<sub>2</sub> protons). <sup>13</sup>C NMR: 141.5 (arom. Ring C), 118.6 (CNH), 163.9 (CNH<sub>2</sub>), 114.3, 112.2, 119.5, 122.5, 123.6, 141.5, 115.2, 118.2 121.5,1248 (CH and C). Anal. Cal. For C<sub>12</sub>H<sub>10</sub>N<sub>2</sub>S: C, 67.25; H, 4.70; N, 13.08; S, 14.97%. Found: C, 67.18; H, 4.50; N, 13.02; S, 14.09%.

### 1-Acetylaminothiazine (9)

In a 100 ml beaker, 3.20 g (0.13 mol) of 1-aminophenothiazine dihydrochloride was added to 30 ml water. The solution was warmed to 50°C and 1.5 ml acetic anhydride added. Aqueous lead acetate prepared from 5 g (0.015 mol) lead acetate in 10 ml water was quickly added to the mixture. The beaker was swirled intermittently and placed in an ice bath for 20 min, filtered and the crystals were washed with cold water, dried and purified by column chromatography (silica gel, DMSO). Yield: 14.80 g (82.31%); m.p. 162-163°C. IR: 3670 (N-H stretch), 2929-2861 (C-H stretch), 979-713 (C-H out of plane), 1462 (C-H in-plane), 1354 (C-N stretch), 1611-1462 (Arom. Skeletal system), 2671 (C=O stretch), 2385 (-CH<sub>2</sub> groups). UV: 262.0 nm. <sup>1</sup>H NMR: 7.29 (d, 1H), 7.09 (d, 2H), 6.97 (d, 6H), 6.84 (d, 7H), 6.83 (d, 8H), 7.20 (d, 9H), 6.53-8.36 (m, NH protons), 3.98-3.94 (s, OCH<sub>3</sub>), 2.19-2.26(s, -CH<sub>3</sub>). <sup>13</sup>C NMR: 144.6 (C aromatic ring), 54.6 (CNH), 55.3 (OCH<sub>3</sub>), 115.6, 113.4, 120.1, 122.6, 124.6, 141.8, 115.10, 118.4, 121.6, 124.9 (CH and C). Anal. Cal. For C<sub>14</sub>H<sub>12</sub>N<sub>2</sub>OS: C,65.76; H,4.70; N,10.88; O,6.21; S,12.45%. Found: C,65.70; H,4.67; N,10.78; O,6.18; S,12.42%.

### 1-Amino-2-Nitrophenothiazine (10)

Powdered 1-acetylaminothiazine (0.41 g, 0.002 mol) was added to glacial acetic acid (0.4 ml) in a 100 ml beaker. While stirring, concentrated sulphuric acid (0.8 ml) was added to the mixture surrounded by a freezing mixture of ice and salt. At 0°C, a cold mixture of concentrated nitric acid (90.2 ml) and was added dropwise. The mixture was held at room temperature for one hour. After cooling to room temperature, the reaction mixture was poured into 500 ml cold water and allowed to cool for 15 min, then filtered with suction in a Buchner funnel and washed with cold water. The filtrate was heated for 2 h to obtain oily product of two layers which were separated to give two isomeric compounds. Purification was by column chromatographic method (Scheme 1). Yield: 210 ml (96.8%). UV: 540 nm. IR: 3698-3100 (hydrogen bonded N-H), 2912 (Ar,C-H); 1370 (Ar, C-N), 1644, 1473 (Aromatic skeleton). <sup>1</sup>H NMR: 7.23 (d, 1H), 6.98 (d, 2H), 6.95 (s,6H), 6.82 (m, 7H), 6.92 (d, 8H), 8.80 (d,9H), 8.30 (m, NH protons), 6.71 (m, NH<sub>2</sub> protons). <sup>13</sup>C NMR: 142.8 (C aromatic ring), 121.7 (CNH), 167.3 (CNH<sub>2</sub>), 130.6 (CNO<sub>2</sub>), 111.6, 112.5, 121.4, 123.2, 126.7, 140.1, 115.2, 117.3, 122.8, 124.1 (CH and C). Anal. Cal. For C<sub>12</sub>H<sub>9</sub>N<sub>2</sub>O<sub>2</sub>S: C, 58.76; H, 3.70; N, 11.42; S,13.07; O, 13.05%. Found: C, 58.72; H, 3.56; N, 11.38; S, 13.02; O, 13.01%.

### 1-amino-4-nitrophenothiazine (11)

Compound 11 was synthesized by using similar method as in 10 above. Yield: 68 ml (31.3%). UV: 490 nm. IR: 3692-3100 (hydrogen bonded N-H), 2899 (Ar. C-H), 1376 (Ar. C-N), 1642, 1472 (Ar. Skeleton). <sup>1</sup>H NMR: 6.80 (d, 1H), 6.20 (d,2H), 7.92 (s,6H), 5.89

(m,7H), 7.32 (d,8H), 7.50 (d,9H), 8.11 (m, NH protons), 6.67 (m ,NH<sub>2</sub> protons), <sup>13</sup>C NMR: 138.6 (C aromatic ring), 119,2 (CNH), 165.5 (CNH<sub>2</sub>), 148.4 (CNO<sub>2</sub>), 112.5, 106.5, 123.4, 132.1, 116.7, 138.6, 116.3, 117.6, 123.9, 120.4 (CH and C ). Anal. Cal. for C<sub>12</sub>H<sub>9</sub>N<sub>2</sub>O<sub>2</sub>S: C, 58.76; H, 3.70; N, 11.42; S, 13.07; O, 13.05%. Found: C, 58.70; H, 3.54; N, 11.30; S, 13.00; O, 13.02%.

### 1,2-diaminophenothiazine trihydrochloride(12)

4 g (0.07 mol) of iron powder was added to a warm suspension of 2-nitro-1-aminophenothiazine (10 ml) in water (40 ml) containing 3 ml concentrated hydrochloric acid. 2 g (0.036 mol) of iron powder was added to the reaction mixture and heated for 50 min in a water bath. The resulting suspension was filtered hot and the filtrate treated with excess concentrated hydrochloric acid. Yield: 290 ml. (94.7%). UV: 312 nm. IR: 3671-3200 (N-H stretch), 809-781 (C-H out of plane), 1051 (C-H in-plane), 1477 (C-N stretch), 1641 and 1477 (Arom. skeletal system). <sup>1</sup>H NMR: 7.29 (d, 1H), 7.09 (d, 2H), 6.97 (d, 6H), 6.84 (d, 7H), 6.83 (d, 8H), 7.20 (d, 9H), 7.60 (m, NH protons), 5.70 (m, NH<sub>2</sub> protons). <sup>13</sup>C NMR: 144.6 (C aromatic ring), 119.5 (CNH), 169.5 (CH<sub>2</sub>), 115.6, 113.4, 120.1, 122.6, 124.6, 141.8, 115.1, 118.4, 121.6, 124.9 (CH and C). Anal. Cal. for: C<sub>12</sub>H<sub>11</sub>N<sub>3</sub>S: C, 63.02; H, 4.81; N, 18.24; S, 13.92%. Found: C, 63.01; H, 4.79; N, 18.22; S, 13.90%.

### 13H-5,14-dihydroquinoxalino[2,3-a]phenothiazine (13)

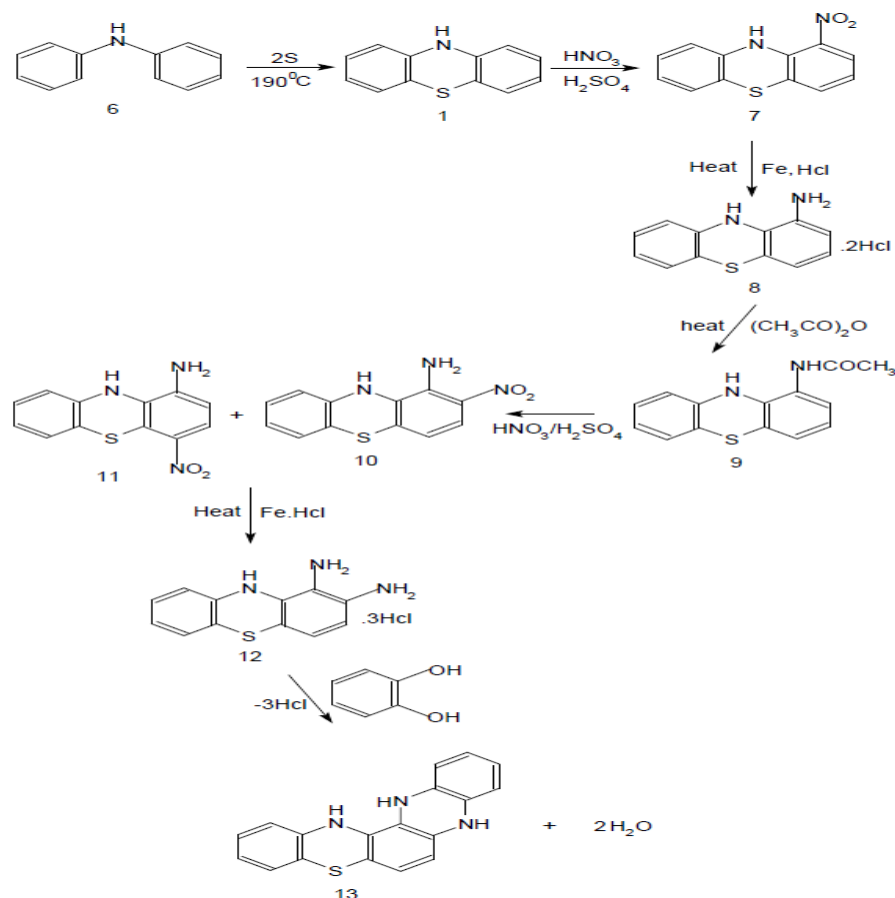
A mixture of 1,2-diaminophenothiazine hydrochloride (10 ml) and catechol (7.5 g, mol) was refluxed with ethanol (30 ml, 3 times for 1 h) and filtered off. The product was dried and purified by column chromatography. Yield: 15.32 g (98.4%). m.p. 174-175°C. UV: 320 nm. IR: 3773 (N-H stretch), 2910-2819 (Ar, C-H), 713 (C-H out of plane bending), 1098 (C-H in plane bend). <sup>1</sup>H NMR: 6.83 (d, 1H ), 7.89 (d, 2H), 7.62 (s, 4H), 5.88 (m, NH protons), 7.29 (dd, 8H), 7.08 (d, 9H), 6.98 (dd, 13H), 6.84 (d, 15H), 7.19(d, 16H), 7.93 (s, 3H), 6.85 (d, 14H).<sup>13</sup>C NMR: 145.7 (C-aromatic ring); 119.7 (CNH), 116.11 (C=C), 126.9, 128.2, 127.3, 127.8, 122.7, 115.8, 116.3, 112.3, 121.1,123.4, 123.9, 142.4, 116.11, 149.3, 122.4, 125.2 ( CH and C). Anal. Cal. For C<sub>20</sub>H<sub>15</sub>N<sub>3</sub>S: C, 72.92; H, 4.59; N, 12.76; S, 9.74%. Found: C, 72.89; H, 4.55; N, 12.57; S, 9.71%.

### Acute toxicity studies

The acute toxicity (LD<sub>50</sub>) was determined following the method described by (Amos et al., 2002; Gurad et al., 2011; Lorke, 1983). Animals were divided randomly into six groups of six mice each. The sample was administered intraperitoneally in the range of doses 10, 100, 1000, 1500, 2000, 3500 and 5000 mg/kg. The animals were observed for 72 h. At the end of the experiment, the animals were sacrificed and then autopsied and examined microscopically for any pathological changes.

### Studies on exploratory activity in mice

Mice were divided into four groups of six mice each. Groups 1 and 2 were treated with sample at doses 50 and 100 mg/kg i.p respectively, while group 3 received normal saline (10 ml/kg) which served as control. Animals in group 4 were treated with diazepam (a known neurosedative) 2 mg/kg i.p (File and Pellow, 1985; Kota et al., 2010). 30 min after the drugs were administered; the animals were placed individually in an automatic Letica board with 16 evenly spaced holes with a counter (Letica LE3333). The number of head dips by the mice into the holes over a period of 5 min was automatically counted (Koofreh et al., 2012; Perez et al., 1998;



**Scheme 1.** Synthetic routes for all the compounds.

Wolfman et al., 1994).

### Studies on spontaneous motor activity

Adult mice were randomly divided into three groups of 6 mice each. Groups 1 and 2 received the sample at doses 50 and 100 mg/kg i.p, while group 3 received normal saline (10 ml/kg p.o). Motor activity of the mice was recorded using a Letica activity cage floor. The animals were singly placed in the cage and their activity was recorded for 6 min at 30 min intervals for a period of 120 min (Odin et al., 2003). In another experiment, the effect of aminophiline 2 mg/kg i.p was recorded. The effects of the sample on aminophiline – induced hyperactivity were compared to that of chlorpromazine 2 mg/kg i.p.

### Studies on pentobarbital induced sleep

Adult rats were divided into 4 groups of 6 rats each. Groups 1 and 2 received 50 and 100 mg/kg i.p of the sample and group 3 was administered normal saline (10 ml/kg p.o) and served as control (Jae-wook et al., 2012; Kaul and Kulerni, 1978; Ngouemo et al., 1994). Diazepam 1 mg/kg i.p was administered to animals in group 4. All the animals were injected with Phenobarbital sodium (phenobarbitone 35 mg/kg), 30 min after the drug treatment. The onset and duration of sleeping time were recorded (Hong et al., 2009; Wambebe, 1985).

### Studies on apomorphine (fortwin) – induced climbing in mice

Adult mice were randomly divided into 3 groups of 10 mice each. The first group received normal saline (10 ml/kg p.o) and served as control. Groups 2 and 3 received the sample at doses of 50 and 100 mg/kg i.p. 30 min after treatment, all mice were treated with apomorphine (fortwin) 3 mg/kg (Hong et al., 2009; Protais et al., 1976). Readings were taken at 10, 20, and 30 min after apomorphine administration. The mice were observed for climbing and scored as follows:

- 0= fore paws on the floor
- 1= fore feet holding the vertical bars
- 2= fore feet holding the bars.

## RESULTS

Phenothiazine (1) was synthesized from the fusion of diphenylamine (6) with excess elemental sulphur. The sulphur residue was removed by heating the mixture after benzene was added and was filtered hot. The filtrate is phenothiazine in benzene which was recovered on heating to dryness. The phenothiazine (1) was nitrated with a mixed acid at 50°C while avoiding polynitration to give 1- nitrophenothiazine (7).

Reduction of (7) with iron in dilute hydrochloric acid furnished 1-aminophenothiazine dihydrochloride (8), which was subsequently reacted with acetic anhydride to achieve (9). This was done to protect the amino group in (8) from further nitration. Nitrating compound (9) in mixed acid yielded ortho and para nitro phenothiazines, (10) and (11) respectively. Reduction of (10) with iron in dilute hydrochloric acid furnished 1,2-diaminophenothiazine trihydrochloride (12), which when added to catechol and refluxed with ethanol gave the novel pentacyclic product: 13H-5,14-dihydroquinoxalino[2,3-a]phenothiazine (13) (Scheme 1).

The structural assignment of the synthesized compounds is based on the spectral data. In the IR spectrum of Compound 1, absorption band at  $2999\text{ cm}^{-1}$  represents the hydrogen bonded N-H stretching. There were number of peaks at  $2859\text{-}2861\text{ cm}^{-1}$ ,  $717\text{ cm}^{-1}$ ,  $1197\text{-}1211\text{ cm}^{-1}$ ,  $1300\text{-}1411\text{ cm}^{-1}$  for aromatic C-H stretching, out of plane C-H bending, in-plane C-H bending and the aromatic C-N stretching respectively. Only two of the aromatic skeletal stretching bands were readily visible at  $1300\text{-}1473\text{ cm}^{-1}$ . The  $^1\text{H}$  and  $^{13}\text{C}$  NMR studies of Compound 1 confirmed the structure. The Compound 1 reacting with mixed acids (nitration) yielded 1-nitrophenothiazine (7). The IR spectrum of compound (7) showed absorption for aromatic C-H stretching and in-plane C-H bending at  $2910$  and  $972\text{ cm}^{-1}$  respectively. The aromatic skeletal system is responsible for the bands at  $1611$  and  $1462\text{ cm}^{-1}$ .

Compound (7) was reduced with iron to give (8)-1-aminophenothiazine dihydrochloride. The N-H stretching and the aromatic C-H stretching appeared at  $3541$ ,  $2819$  and  $2821\text{ cm}^{-1}$  respectively. The in-plane C-H band appeared weakly at  $1093\text{ cm}^{-1}$ , while the C-N stretching showed at  $1320\text{ cm}^{-1}$  which is characteristic of aromatic amines. The bands at  $1684$  to  $1698\text{ cm}^{-1}$  are that of aromatic skeletal system. In  $^1\text{H}$  NMR spectra data, Compound (7) shows a singlet at  $\delta$  10.30 to 9.81 due to N-H proton. This was shifted to  $\delta$  9.76 in 1-aminophenothiazine hydrochloride (8). This shifting towards upfield in compound 8 is ascribed to intramolecular hydrogen bonding as  $\text{-NH}\dots\text{O}=\text{N}$  in Compound 7.

Compound (8) was subsequently reacted with acetic anhydride to protect the amino group from further nitration. This yielded 1-acetylaminophenothiazine (9). The hydrogen bonded N-H stretching appeared at  $3670\text{ cm}^{-1}$ , while the bands at  $2929$  and  $2861\text{ cm}^{-1}$  were for C-H stretching for aromatic systems. The bands at  $1354\text{ cm}^{-1}$  is characteristic of aromatic C-N stretching, while bands at  $2385$  and  $2671\text{ cm}^{-1}$  indicated C=O stretching and methylene  $\text{CH}_2$  groups. In the  $^1\text{H}$  NMR spectrum of Compound 9, the multiplet for  $\text{-NH}$  protons appeared in the region  $\delta$  6.53 to 8.36. The  $\text{-OCH}_3$  protons and  $\text{-CH}_3$  protons in the compound showed a singlet in the region  $\delta$  3.98-3.94 and  $\delta$  2.19 to 2.26 respectively, indicating a complete acylation of Compound 8.

The nitration of Compound (9) yielded two isomers: 2-nitro-1-aminophenothiazine and 4-nitro-1-aminophenothiazine (Compounds 10 and 11 respectively). The IR spectra of compounds 10 and 11 showed broad bands at  $3698$  to  $3100\text{ cm}^{-1}$  indicating hydrogen bonded N-H stretching. The absorption band at  $2912\text{ cm}^{-1}$  was for aromatic C-H stretching. The band at  $1370\text{ cm}^{-1}$  is characteristic of aromatic C-N stretching, while the aromatic skeletal was found at  $1644\text{ cm}^{-1}$  and  $1473\text{ cm}^{-1}$ . Similarly, in compound 10, N-H<sub>2</sub> proton appeared as multiplet at  $\delta$  6.71, while in  $^{13}\text{C}$  NMR spectrum, a characteristic signal appeared for  $(\text{CNH}_2)$  and  $(\text{CNO}_2)$  in the range of  $\delta$  167.3 and  $\delta$  130.6 respectively. These were found absent in compound 9 indicating a successful nitration of this compound. The nitro group is responsible for the broad shoulder at  $1195\text{ cm}^{-1}$ .

Reduction of (10) furnished 1,2-diaminophenothiazine hydrochloride (12). The IR spectrum of (12) showed a broad band at  $3671$  to  $3200\text{ cm}^{-1}$  for hydrogen bonded N-H stretching. The band at  $1477\text{ cm}^{-1}$  indicated C-N stretching, while the aromatic skeletal system was located at  $1641$  and  $14777\text{ cm}^{-1}$ . In the  $^1\text{H}$  NMR spectrum, Compound 12 showed two signals for NH and NH<sub>2</sub> at  $\delta$  7.60 to 5.70 respectively. A characteristic signal appeared for CH<sub>2</sub> in the range of  $\delta$  119.5 in the  $^{13}\text{C}$  NMR spectrum, while that of CNH<sub>2</sub> was located at  $\delta$  169.5.

Refluxing a mixture of Compound (12) and catechol with ethanol yielded the pentacyclic product-13H-5,14-dihydroquinoxalino[2,3-a]phenothiazine (13). The IR spectrum of Compound (13) showed N-H stretching at  $3773\text{ cm}^{-1}$ . The bands at  $2910$  to  $2819\text{ cm}^{-1}$  appeared for aromatic C-H stretching, while bands at  $713$  and  $1098\text{ cm}^{-1}$  were for C-H out-of-plane bending and in-plane bending respectively. These clearly support the fact that Compound (11) was not used in the synthesis of the novel product (13). The absorption at  $205\text{ nm}$  in the UV-visible spectrum of Compound (1) resembles that of benzene while the shift in wavelength to  $311\text{ nm}$  indicated the presence of auxochrome type  $\text{-NHR}$  in phenothiazine.

The UV spectrum of (8) showed maximum absorption at  $312\text{ nm}$ . No appreciable bathochromic shift because the compound is in the form of hydrochloride. Compound (10) showed a UV maximum at  $540\text{ nm}$ . This powerful bathochromic shift is probably due to the presence of free amino group, while the pentacyclic product (13) exhibited a UV maximum at  $320\text{ nm}$  characteristic of phenothiazine systems. In the  $^1\text{H}$  NMR spectrum, compound 13 displayed a signal at  $\delta$  5.88 for NH protons, while the multiplet for aromatic protons appeared in the region between  $\delta$  6.54-8.36. In  $^{13}\text{C}$  NMR spectrum of compound 13, a characteristic signal appeared for  $(\text{CNH})$  in the range of  $\delta$  119.7. The mass spectrophotometric studies performed on the phenothiazines confirmed the molecular weight values. The results of the pharmacological tests are as presented in Tables 1, 2, 3, 4 and 5.

**Table 1.** Effect of sample on exploratory activity in mice.

Treatment	Dose mg/kg	Mean score
Normal saline	10 ml/kg	40.8±5.8
Sample	50	21.3±2.4
Sample	100	12.2±2.9
Diazepam	2	15.0±3.5

**Table 2.** Effect of sample on spontaneous motor activity in mice.

Treatment	Dose mg/kg	Time (minutes)				
		0	30	60	90	120
Normal saline	10 ml/kg	91.2± 3.6	86.2± 2.5	82.8± 1.8	81.8± 2.0	75.5± 2.8
Sample	50	91.8±4.1	35.8±3.1	31.8± 2.3	22.5± 2.8	13.7±2.0
Sample	100	90.7± 1.2	33.0± 2.4	14.7± 1.7	8.2± 1.3	5.8±1.1

**Table 3.** Effect of sample on aminophillin induced hypermotility in mice.

Treatment	Dose mg/kg	Time (minutes)				
		0	30	60	90	120
Normal saline	10 ml/kg	90.3±2.9	85.2± 2.5	82.5±2.4	81.0±1.5	76.0± 2.9
Aminophillin	2	90.0±1.6	102.1±4.4	126±5.2	118±3.1	104 ±2.9
Aminiphillin + sample	50	91.8±1.6	73.5±2.9	53.5±2.6	33.7±3.1	17.3±2.7
Aminophillin +sample	100	90.5±2.2	62.5±2.2	34.2±2.4	17.3±2.6	14.7±2.5

## DISCUSSION

The structural assignment of the synthesized compounds was based on the spectral data. The IR spectrum of the pentacyclic Compound (13) clearly showed that the isomeric Compound (11) was not used in the synthesis of the final product. This was further buttressed by the disappearance of C-O absorption ( $1200\text{ cm}^{-1}$ ) in the spectrum of (13). The pentacyclic product exhibited a UV maximum at 320 nm characteristic of phenothiazine systems. The angular pentacyclic ring system was further identified by the information from the  $^1\text{H}$  and  $^{13}\text{C}$ NMR spectral with the resonances assigned to hydrogen and carbon. Compound **13** (sample) when administered, inhibited the exploratory behaviour in mice dose dependently. The effect was similar to that of diazepam (2 mg/kg), a known neurosedative and significantly different from those of control (Table 1). From Table 2, at 50 and 100 mg/kg i.p, the sample caused a significant time and dose dependent decrease in the spontaneous motor activity in mice.

Similarly, aminophillin induced hypermotility was reduced dose and time dependently (Table 3). When aminophillin alone is administered, at 60 min the mice was very active,  $12\pm 5.2$ , while the combination of 50

mg/kg sample with aminophillin reduced the activities of the mice,  $53.5\pm 2.6$ . The activities of the mice were further reduced,  $34.2\pm 2.4$  when the dose was increased to 100 mg/kg. Similarly at 120 min, it was noticed that at 50 mg/kg the activities of the mice reduced to  $17.3\pm 2.7$ , while 100 mg/kg sample plus aminophillin further reduced the activities of mice to  $14.7\pm 2.4$ . Table 4 recorded that the administration of the sample at 50 and 100 mg/kg i.p did not affect the onset of sleep, but significantly prolonged the duration of pentobarbital sleep dose dependently. Similarly, Table 5 showed that 50 and 100 mg/kg administered i.p inhibited fortwin induced climbing dose dependently.

## Conclusion

The importance of linear phenothiazine compounds as antipsychotic drugs has long been recognised. Compound **13** is the first angular pentacyclic phenothiazine to possess neurosedative properties. The hole board experiment is a measure of exploratory activity and a decrease in this parameter revealed sedative effects. The procedure has been accepted as a parameter for evaluating anxiety condition. The decrease

**Table 4.** Effect of sample on pentobarbital induced sleep in mice.

Treatment	Dose{(mg/kg)}	Duration of sleep (minutes)
Normal saline	10 ml/kg	52.6±4.2
Sample	50	92.8± 5.6s
Sample	100	126±2.6
Diazepam	1	82.8±3.4

**Table 5.** Effect of sample on fortwin induced climbing in mice.

Treatment	Time (minutes)		
	1 0	20	30
normal saline 10ml/kg	0	1	2
Sample 50 mg/kg	1	0	0
Sample 100 ml/kg	0	0	0

The values are expressed as follows: 0= four paws on the floor, 1= fore feet holding the vertical bars, 2= fore feet holding the bars.

in spontaneous motor activity and potentiation of pentobarbital induced sleep strongly suggest central depressant activity. The ability of Compound **13** to antagonise fortwin - induced climbing behaviour in mice has been correlated with neuroleptic potential.

## ACKNOWLEDGEMENT

The authors are grateful to Chemistry Laboratory, Kogi State University for the spectroscopic and elemental analysis and Paul Ojodale Samuel for Secretarial assistance.

## REFERENCES

- Abdel-Monem MM, Portoghese PS (1972). Medical Chemistry, Hampton Press, N. Y., USA. pp.16/208.
- Abdel-Rahman A, Kandeel E, Berghot M, Mauwa A (2013). Synthesis and Reactions of Some new Benzo[a]phenothiazine-3,4-dione Derivative. J. Het. Chem. 50:298-303.
- Alan RK, Samia A, Baozhen Y, Guotang Q (1999). Synthesis of Tetracyclic and Pentacyclic Phenothiazine via Benzotriazole Methodology. J. Het. Chem. 36:473.
- Amos S, Binda A, Vongtan H, Odin EM, Okwute SK (2002). Sedative effect of the methanolic leaf extract of *Newbouldia Leavis* in mice and rats. Boll. Chim. Farmac 144(6):471– 475.
- Chuan D, Xiaofei S, Xingzhao T, Li W, Dan Z (2012). Synthesis of Phenothiazines via Ligand-free CuI-catalyzed cascade C-S and C-N Coupling of aryl ortho-dihalides and ortho-aminobenzenethiols. Chem. Comm. 48:5367-5369.
- Ezema B, Okafor C, Ezema C, Onoabedje A (2012). Synthesis of New Diaza Angular and Tetraaza Complex Phenothiazine Rings. Chem. Pro. Eng. Res. 3:107-119.
- File S, Pellow S (1985). The effect of Triazolobenzodiazepines in TWO Animals of Anxiety on the hole board. Brit. J. Pharm. 86:729–735.
- Gurad A, Anshoo G, Pravin K, Abdesh K (2011). Acute Toxicity Studies of Safer and more effective Analogues of N,N-Diethyl-2-Phenylacetamide. J. Med. Entomol. 48(6):1160-1166.
- Hong M, Chung-soo K, Yuan M, Ki-wan O (2009). Magnold Enhances Pentobarbital-induced Sleeping Behaviours: Possible involvement of GABAergic Systems. Phyto. Res. 23(9):1340-1344.
- Jae-wook K, Chung-soo K, Zhenzhen H, Ki-wan O (2012). Enhancement of Pentobarbital- induced Sleep by Apigenin through Chloride Ion Channel Activation. Arch. Pharm. Res. 35(2):367-373.
- Kaul PN, Kulkarni SK (1978). New Drug Metabolism Inhibitor of Marine Origin. J. Pharm. Sci. 67:1293–1296.
- Koofreh D, Christopher E, Justina N, Atim A (2012).: Locomotor and Exploratory Behaviour in Mice with Treated Oral Artemether Suspension. Sci. Acad. Pub. 1(3):17-24.
- Kota T, Shozo T, Nobuhiro N (2010). Decreased Exploratory Activity in a Mouse Model of 15 q duplication Syndrome. J. PLOS ONE 5:12.
- Lorke D (1983). A new approach to practical acute toxicity. Arch. Toxicol. 54:25–27.
- Luiza G, Castelia C, Clavdia M, Loan A (2007). Microwave Assisted Synthesis of Phenothiazine and Quinoline Derivatives. Int. J. Mol. Sci. 8(2):70-80.
- Martina H, Jan S, Anthony J, Kenneth I, Thomas J, Uwe H (2007). Phenthiazine Synthesis and Metallochromic Properties. J. Org. Chem. 72(18): 6714-6725.
- N'gouemo P, Nguemby-Bina C, Baldy-Moulinia M (1994). Some Neuropharmacological effect of an Ethanolic Extract of *Mapronnea* African in Rodents. J. Ethno. 43:161–166.
- Odin EM, Okwute SK, Amos S, Gamaliel K (2003). Antimalarial and Neurosedative Properties of *Newbouldia Laevis* leaf. Int. Wd. J. Sci. Tech. 2(1):18–97.
- Okafor CO (1978). A New Synthesis of Three – Branched Diazaphenothiazine Dyes. Dye Pig. 9:427–442.
- Okafor CO (1971). The Chemistry of Natural Products. Int. J. Sulph. Chem. 6B:237.
- Okoro UC, Onoabedje E, Odin EM (2009). The first Angular Triazaphenothione and the related diaza – analogue. Int. J. Chem. 19(4):197–221.
- Perez GRM, Perez IJA, Gacia D, Sossa MH (1998). Neuropharmacological activity of Solanum Nigrum Fruit. J. Ethno. 62:43.
- Protais P, Costertin J, Schwartz JC (1976). Climbing behaviour induced by Apomorphine in Mice. A simple test for the study of dopamine receptors in the stratum. J. Psycho. 50:1-6.
- Tim M, Daniel O, Andrea P, Karl K, Thomas J (2012). Phenothiazinyl Rhodanylidene Merocyanines for Dye-sensitized Solar Cells. J. Org. Chem. 8:300-307.
- Ujuwala S, Meghasham N, Mahendra C (2012). Synthesis,

- characterization and antimicrobial activity of some 2-(propenone) aryl 3-substituted phenothiazine. *Der Pharm. Chem.* 4(3):967–971.
- Wambebe C (1985). Influence of some agent that Affect 5-HT metabolism and receptors and nitrazepam induced sleep in mice. *Brit. J. Pharm.* 84:185–191.
- Whitaker R (2004). The case against antipsychotic drugs – A 50 year record of doing more harm than good. *Med. hypo.* 62(1):5–13.
- Wolfman C, Viola H, Paladini AC, Dajas D, Medina J (1994). Possible anxiolytic effects of chrysin, a central benzodiazepine receptor ligand isolated from *Passiflora cocruica*. *Pharm. Biochem. Behav.* 47: 1.

Full Length Research Paper

## Quantum chemical calculations on molecular structures and solvents effect on 4-nitropicolinic and 4-methoxypicolinic acid

Semire Banjo\* and Adeoye Idowu Olatunbosun

Department of Pure and Applied Chemistry, Faculty of Pure and Applied Sciences, Ladoke Akintola University of Technology, P. M. B. 4000, Ogbomoso, Oyo State, Nigeria.

Accepted 08 July, 2013

The density functional theory (DFT) (B3LYP) was used to study the solvents effect on electronic properties of 4-methoxypicolinic acid (4MOPIC) and 4-nitropicolinic acid (4NPIC). The calculated vibration frequencies at DFT/6-311++G\*\* were compared to that of un-substituted picolinic acid to know the effect of donor/acceptor substituent on the molecules. Five solvents namely acetone, ethanol, diethyl ether, N, N-dimethylformamide (DMF) and tetrahydrofuran (THF) were used to study solvents effect. The methoxyl (OCH<sub>3</sub>) group in 4MPIC pushed electrons into the picolinic acid ring thereby resulted in upfield resonance as compared to 4NPIC in which nitro (NO<sub>2</sub>) group brought about downfield in <sup>1</sup>HNMR. The solvents increased the minimum energy required to remove an electron for 4MOPIC whereas it was lower in 4NPIC. The HOMO and LUMO energies calculated in the solvents revealed that both HOMOs and LUMOs experienced stabilization in 4NPIC but LUMOs were destabilized in 4MOPIC as compared to gas phase.

**Key words:** 4-methoxypicolinic acid, 4-nitropicolinic acid, solvents effect, density functional theory (DFT).

### INTRODUCTION

Picolinic acid and its substituents are of interest to many researchers mainly because of their usefulness as ligands; the availability of some donor atoms on the compounds which can serve as binding sites to various metals in forming various monomeric and polymeric complexes (Yurovskaya et al., 1998). Picolinic acid is the body's prime natural chelator of vital trace elements such as chromium, zinc, manganese, copper, iron and molybdenum (Evan and Johnson, 1980). Picolinic acid is biosynthesized in the liver and kidneys from the amino acid tryptophan, and stored in the pancreas during digestion, secreted into the intestine (Fernandez-Poi et al., 2001).

The vibrational frequencies, UV-Visible, <sup>1</sup>H and <sup>13</sup>C NMR spectra of picolinic acid with its metal complexes of Fe(III), Ni(II), Cu(II), Zn(II) and Ag(I) were recently

reported (Kalinowska et al., 2007; Goher and Abu-Youssef, 1996). The 3-methylpicolinic acid and 6-methylpicolinic acid with their cobalt complexes were synthesized and characterized by spectroscopic techniques and thermal characterization in the solid state (Kukovec et al., 2009).

In the past the chemical behaviour of ambident ligands such as mercaptobenzothiazole and mercaptobenzimidazole ligands has been investigated using density functional theory (AlHokbany and AlJammaz, 2011). This is with a view of understanding the coordination chemistry of the metal complexes to be formed. Density functional theory has been employed over the years to obtain thermochemical data, molecular structure force fields frequencies assignment of nuclear magnetic resonance (NMR), photoelectron, erythrocyte

\*Corresponding author. E-mail: bsemire@lautech.edu.ng.

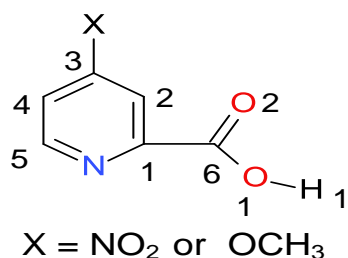


**Figure 1.** Schematic structures of the studied molecules: 4-nitropicolinic acid for X = NO<sub>2</sub> and 4-methoxypicolinic acid for X = OCH<sub>3</sub>.

sedimentation rate (ESR) and ultra violet (UV) spectra, activation barriers, dipole moments and other one electron properties (Koczon et al., 2003; Parajón-Costal et al., 2004; Ziegler, 1991).

The effect of protic and aprotic solvents on the reactivity of picolinic, nicotinic and isonicotinic acid as well as of some substituted nicotinic acids with diazodiphenylmethane has been investigated (Dimitrijević et al., 1974; Drmanic et al., 2012; Marinkovi, 2005). In one of our recent work, DFT/B3LYP with various basis sets (6-31G\*, 6-31G\*\*, 6-311G\*\*, 6-311+G\*\*, 6-311++G\*\*) was used to study solvents effect on geometry and electronic properties of picolinic acid. The results revealed that solvent-molecule interactions are more prominent around the heteroatoms in the case of the polar solvents. Therefore, this was a greater shielding/de-shielding on carbon nuclei around nitrogen and oxygen atoms of picolinic acid in the case of the polar solvents (Adeoye and Semire, 2013). The aim of this study is to employ density functional theory to study the effect of solvents on molecular structures and electronic properties of two 4-substituted picolinic acid namely 4-nitropicolinic acid and 4-methoxypicolinic acid as shown in Figure 1. The solvents employed are acetone, Ethanol, Diethyl ether, N,N-Dimethylformamide (DMF) and Tetrahydrofuran (THF) (Figure 1).

## COMPUTATIONAL METHODS

The 4MOPIC and 4NPIC were optimized without symmetry constraint using density functional theory Beckes's three-parameter hybrid functional (Becke, 1988) employing the Lee, Yang and Parr correlation functional B3LYP (Lee et al., 1988) with 6-31G\*, 6-31G\*\* and 6-311G\*\* basis sets. The vibration frequencies, electronic properties and NMR were calculated. In the calculation of vibration frequency, no imaginary frequency modes were obtained for the two molecules, therefore it was believed that true minimum on the potential energy surface were found for the molecules. The absorption transitions were calculated from the optimized geometry in the ground state S<sub>0</sub> using configuration interaction (CI) theory using density functional theory (DFT with 6-31G\* in five different solvents namely acetone, ethanol, diethyl ether, N,N- Dimethylformamide (DMF) and tetrahydrofuran (THF). The convergence criteria for the energy calculations and geometry

optimizations used in the density functional methods were default parameters in the Spartan 06 program (Table 1).

## RESULTS AND DISCUSSION

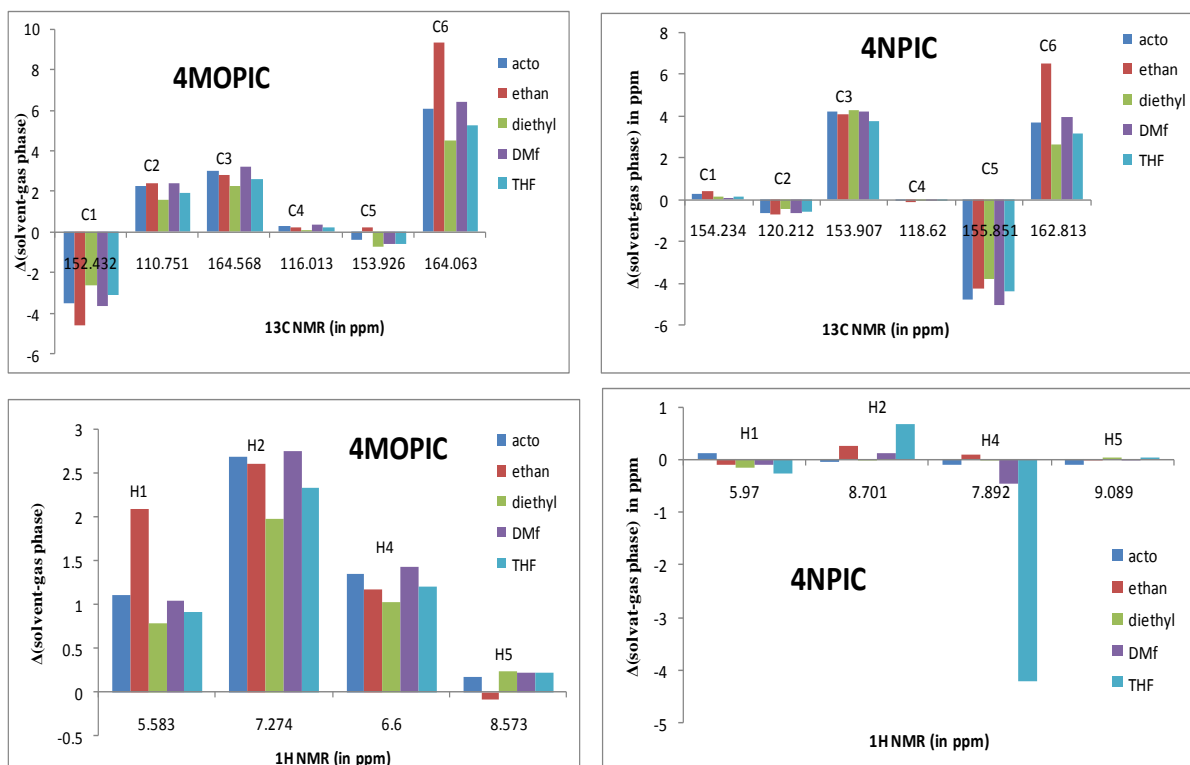
### Chemical shifts and solvents effect

The molecular structure of the optimized 4MOPIC and 4NPIC using B3LYP method with 6-31G\* basis set is used to calculate <sup>13</sup>C and <sup>1</sup>H chemical shift calculations as shown in Table 1. It has been reported that <sup>13</sup>C and <sup>1</sup>H NMR calculated using DFT are in good agreement with the experimental values (Teimouri et al., 2008; Karakurt et al., 2012; Cheeseman et al., 1996). Therefore, in the absence of experimental results the calculated <sup>13</sup>C and <sup>1</sup>H NMR using DFT method can provide reasonable information that could assist in structural elucidation; thus the chemical shifts of the two isomers are compared. The results in Table 1 showed that <sup>13</sup>C NMR chemical shifts for the two molecules are greater than 100 ppm which is the typical <sup>13</sup>C NMR chemical shift for organic molecule (Kalinowski et al., 1988; Pihlaja and Kleinpeter, 1994). It has been reported that calculations based on the averaging of chemical shifts are in better agreement with the experimental values than plain calculations using optimized geometry (Stare et al., 2004). The chemical shifts of C2 and C4 are 109.373 and 115.541 ppm for 4MOPIC and 119.611 and 118.174 pmm for 4NPIC, therefore C2 and C4 experienced shielding effect because of its position in the molecules whereas other carbon atoms are de-shielded. C2 and C4 are more shielded in 4MOPIC because of higher electron density as a result of electron donating effect of CH<sub>3</sub> substituent. The chemical shifts of C3 are 165.388 and 155.204 ppm for 4MOPIC and 4NPIC respectively. The shielding/de-shielding of the substituent has no effect on C1, C5 and C6 of 4MOPIC as compared to un-substituted picolinic acid (Adeoye and Semire, 2013), although C1 and C5 in 4NPIC are slightly de-shielded. This is in agreement that the presence of electronegative atom attracts all electron clouds of carbon atoms towards itself, which in turn leads to de-shielding of carbon atoms and results in increase in chemical shift values (Varsanyi and Sohar, 1972). This de-shielding effect is noticed in 4NPIC molecule because of the attachment of NO<sub>2</sub> group.

The aromatic proton signals are observed at 5 to 7 ppm (Kalinowski et al., 1988; Pihlaja and Kleinpeter, 1994) and it has been found that presence of electrons on aromatic ring, double bonded atoms, and triple bonded atoms has been found to de-shield attached hydrogen (Varsanyi and Sohar, 1972). Its chemical shifts would be more susceptible to intermolecular interactions as compared to that for other heavier atoms. The methoxyl (OCH<sub>3</sub>) group in 4MPIC pushed electrons into the picolinic acid ring thereby results in upfield resonance as compared to 4NPIC in which nitro (NO<sub>2</sub>) group brought about downfield (Table 1). For instance, chemical shifts

**Table 1.**  $^{13}\text{C}$  NMR and  $^1\text{H}$  NMR (ppm) calculated at DFT/B3LYP level with various basis.

Atom	4-methoxypicolinic acid				4-nitropicolinic acid			
	6-31G*	6-31G**	6-311G**	Aveg.	6-31G*	6-31G**	6-311G**	Aveg.
C1	152.432	145.375	154.018	150.608	154.234	147.115	155.407	152.252
C2	110.751	105.608	111.760	109.373	120.212	115.441	123.179	119.611
C3	164.568	158.971	172.625	165.388	153.907	150.061	161.643	155.204
C4	116.013	110.919	119.691	115.541	118.620	114.036	121.866	118.174
C5	153.926	145.624	155.270	151.607	155.851	147.514	156.685	153.350
C6	164.063	154.569	165.406	161.346	162.813	153.348	164.105	160.089
H1	5.583	6.757	5.511	5.950	5.970	7.166	5.868	6.335
H2	7.274	8.616	7.404	7.765	8.701	10.015	8.826	9.181
H4	6.600	7.867	6.862	7.110	7.892	9.198	8.015	8.368
H5	8.573	9.733	8.747	9.018	9.089	10.261	9.247	9.532

**Figure 2.** Solvents effect on  $^{13}\text{C}$  NMR and  $^1\text{H}$  NMR in ppm calculated at DFT/6-31G\* level.

for H2 and H4 are 7.765 and 9.018 ppm for 4MOPIC and 9.181 and 9.532 ppm for 4NPIC respectively. The hydroxyl oxygen atom shows electronegative property hereby contributed to hydroxyl hydrogen atom (H) downfield resonance as reflected in the two molecules. The calculated chemical shifts of hydroxyl hydrogen atom are 5.950 and 6.355 ppm for 4MOPIC and 4NPIC respectively which shows that  $\text{NO}_2$  substituent increased downfield resonance experienced by hydroxyl hydrogen atom of 4NPIC (Table 1).

Theoretically, the solvent effect is estimated by comparing calculated chemical shifts for solution and gas phase at a particular level of calculation. In this work, the  $^{13}\text{C}$  NMR and  $^1\text{H}$  NMR calculated at DFT/6-31G\* are used to estimate effect of solvents on chemical shifts as shown in Figure 2. The effects of solvents on  $^{13}\text{C}$  NMR chemical shifts for 4MOPIC are pronounced on C1, C2, C3 and C6. For instance, the differences calculated on C6 for 4MOPIC as compared to gas phase are 6.086, 9.301, 4.503, 6.379 and 5.256 ppm for acetone, ethanol, diethyl

**Table 2.** Selected vibrational frequencies calculated at B3LYP/6-311++G\*\*.

4-methoxypicolinic acid			4-nitropicolinic acid		
Cal.	Int.	Assign.	Cal.	Int.	Assign.
3773	96.50	vOH	3773	115.25	vOH
3242			3246		
3204		vCH	3229		vCH
3160			3171		
1821	353.81	vC=O	1828	346.81	vC=O
1623	244.52		1651	40.40	vC=C +vC=N
1606	21.09		1604	28.18	vC=C +vC=N
1516		vC=C +vC=N	1595	251.34	vC=C +vC=N
1427	5.27	C=C + $\pi$ CH	1495		vC=N + $\pi$ CH
1355	110.82	C-O + $\pi$ OH	1415		vC=C + $\pi$ CH
1334	96.35	vC=N +C-OCH <sub>3</sub>	1375	199.19	vNO <sub>2</sub>
1317	30.00	vC-C + C-N	1360	79.29	C-O + $\pi$ OH
1285	71.94	vC-OCH <sub>3</sub> + $\pi$ OH	1311		C-N + $\pi$ OH+ $\pi$ CH
1177	182.74	$\pi$ CH + $\pi$ OH	1301	30.91	vC=C-C=N+ $\pi$ OH
1134	138.25	$\pi$ CH + C-O	1206	87.52	vC-O + $\pi$ OH +vC-NO <sub>2</sub>
1083	99.00	$\pi$ CH + C-O	1139	203.08	vC-O+ $\pi$ CH
1058	7.26	vC-OCH <sub>3</sub>	1087	71.93	vC-O+ $\pi$ CH
1008	58.98	$\delta$ Ring	1012		$\omega$ Ring
998, 890, 860		$\sigma$ CH	1001, 948, 880		$\sigma$ CH
805		$\pi$ (C=C-C)	734		$\pi$ (C=C-C)
613		$\sigma$ OH	660		$\phi$ (COOH)
572		$\omega$ Ring	608		$\sigma$ OH
262		$\gamma$ CH <sub>3</sub>	276		$\omega$ Ring
207		$\gamma$ CH <sub>3</sub>	345		$\delta$ Ring
186		$\omega$ Ring	146		$\gamma$ Ring
102		$\gamma$ O-CH <sub>3</sub>	37		$\gamma$ (NO <sub>2</sub> + COOH)
36		$\gamma$ COOH			

v, stretching;  $\pi$ , in-plane bending;  $\sigma$ , out-of-plane bending;  $\tau$ , torsion,  $\delta$ , breathing;  $\omega$ , wagging;  $\gamma$ , rocking;  $\phi$ , scissor.

ether, DMF and THF respectively. The effect of ethanol is felt more on C6 and C1 for 4MOPIC molecule (Figure 2). In case of 4NPIC, the solvent effects are pronounced on C3, C5 and C6. For C6, the differences calculated are 3.713, 6.562, 2.681, 3.961 and 3.169 ppm for acetone, ethanol, diethyl ether, DMF and THF respectively as compared to results from gas phase calculations.

The effects of solvents on <sup>1</sup>HNMR chemical shifts for 4MOPIC are felt by all hydrogen atoms although more on H1, H2 and H4. For 4NPIC, the only solvent that has much effect on the molecule is THF as it is reflected in <sup>1</sup>HNMR on H2 and H4. The differences in chemical as compared to gas phase calculation could be explained in terms of changes in free energy hypersurface of the nuclei (Jernej et al., 2004).

### Vibration frequencies

The vibration frequencies calculated at B3LYP/6-

311++G\*\* are shown in Table 2. The ring carbon hydrogen stretching vibrations calculated at B3LYP/6-311++G\*\* are in the region 3242-3160 cm<sup>-1</sup> for 4MOPIC and 3246-3171 cm<sup>-1</sup> for 4NPIC. The C=O stretching vibration for 4MOPIC and 4NPIC are calculated to be 1821 and 1826 cm<sup>-1</sup> with 353.81 and 346.81 intensities respectively. However, C=O stretching vibration for un-substituted picolinic acid was calculated to be 1820 cm<sup>-1</sup> (Adeoye and Semire, 2013) and experimentally observed at 1717 cm<sup>-1</sup> (Varsanyi and Sohar, 1972) and 1719 cm<sup>-1</sup> (Gfeller et al., 1976). The OH stretching vibration is calculated for both molecules at 3773 cm<sup>-1</sup> with  $\approx$  20% higher intensity in 4NPIC. This has been calculated at 3770 cm<sup>-1</sup> and experimentally observed at 3437 and 3464 cm<sup>-1</sup> for un-substituted picolinic acid (Varsanyi and Sohar, 1972; Gfeller et al., 1976). The C=C stretching coupled with C=N are calculated at 1623, 1606 and 1516 cm<sup>-1</sup> for 4MOPIC and 1651, 1604 and 1595 cm<sup>-1</sup> for 4NPIC. The C=C stretching coupled with C-H in plane deformation ( $\pi$ CH) are calculated to be 1427 and 1415 cm<sup>-1</sup> for

4MOPIC and 4NPIC respectively, this has been calculated at  $1462\text{ cm}^{-1}$  and observed at  $1439\text{ cm}^{-1}$  (Varsanyi and Sohar, 1972) and  $1443$  and  $1719\text{ cm}^{-1}$  (Gfeller et al., 1976) for the un-substituted picolinic acid. The C-O stretching coupled with OH in plane deformation ( $\pi\text{OH}$ ) is calculated at  $1355$  and  $1360\text{ cm}^{-1}$  for 4MOPIC and 4NPIC respectively. Also, this has been calculated at  $1358\text{ cm}^{-1}$  and observed experimentally at  $1370$  and  $1347\text{ cm}^{-1}$  (Adeoye and Semire, 2013; Varsanyi and Sohar, 1972; Gfeller et al., 1976) un-substituted picolinic acid. The in-plane bending of C=C-C is calculated at  $805\text{ cm}^{-1}$  for 4MOPIC and  $734\text{ cm}^{-1}$  for 4NPIC.

The C-H out-of-plane deformation ( $\sigma\text{CH}$ ) for 4MOPIC is calculated at  $998$ ,  $890$  and  $860\text{ cm}^{-1}$  whereas this is calculated at  $1001$ ,  $948$  and  $880\text{ cm}^{-1}$  for 4NPIC. The OH out-of-plane deformation ( $\sigma\text{OH}$ ) is calculated to be  $613$  and  $608\text{ cm}^{-1}$  for 4MOPIC and 4NPIC respectively. The COOH rocking vibration was at  $36\text{ cm}^{-1}$  for 4MOPIC and  $37\text{ cm}^{-1}$  for 4NPIC which is coupled with  $\gamma\text{NO}_2$ .

### Global electrophilicity and Electronic properties

The electronic properties of the 4MOPIC and 4NPIC are calculated from the total energies and the Koopmans' theorem. The ionization potential (IP) is determined from the energy difference between the energy of the compound derived from electron transfer which is approximated;  $\text{IP} \approx -E_{\text{HOMO}}$  while the electron affinity (EA) is given as;  $\text{EA} \approx -E_{\text{LUMO}}$ , respectively. The chemical potential ( $\mu$ ), chemical hardness ( $\eta$ ), electrophilicity index ( $\omega$ ) and softness ( $1/\eta$ ) of a molecule are deduced from IP and EA values (Takusagawwa and Shimada, 1976; Zhou and Navangul, 1990; Chamizo et al., 1993; Koopmans, 1734; Parr et al., 1999) as shown in the following Equations 1, 2 and 3.

$$\mu = \left(\frac{\partial E}{\partial N}\right) v(r) \approx -\left[\frac{\text{IP}+\text{EA}}{2}\right] \approx -\left[\frac{E_{\text{HOMO}}+E_{\text{LUMO}}}{2}\right] \quad (1)$$

$$\eta = \left(\frac{\partial^2 E}{\partial N^2}\right) v(r) \approx \left[\frac{\text{IP}-\text{EA}}{2}\right] \approx [E_{\text{HOMO}} - E_{\text{LUMO}}] \quad (2)$$

$$\omega = \frac{\mu^2}{2\eta} \quad (3)$$

It is well known that when IP is small and EA is large and positive the molecule should be soft, therefore soft molecules are often more chemically reactive than hard molecules. Also, the electrophilicity index has being a useful structural depictor of the analysis of the chemical reactivity of molecules (Pearson, 1993; Bird, 1997; Chattaraj et al., 2003; Semire and Odunola, 2013; Semire, 2013). According to the definition, electrophilicity index measures the propensity of a species to accept electrons. As Domingo et al (Domingo et al., 2002) proposed the high nucleophilicity and electrophilicity of

heterocycles corresponds to opposite extremes of the scale of global reactivity indexes. A good, more reactive, nucleophile is characterized by a lower value of  $\mu$ ,  $\omega$  and in opposite a good electrophile is characterized by a high value of  $\mu$ ,  $\omega$ . The electronegativity and hardness are of course used extensively to make predictions about chemical behavior and these are used to explain aromaticity in organic compounds (De Proft and Geerlings, 2001). A hard molecule has a large HOMO–LUMO gap and a soft molecule has a small HOMO–LUMO. The LUMO represents electron(s) accepting ability and HOMO as electron donating ability of a molecule.

The HOMO, LUMO, energy band gap, dipole moment, energy of solvation, chemical potential, softness, electrophilicity/nucleophilicity index and UV-Vis adsorption maximum calculated are displaced in Table 3. The values of chemical hardness, chemical potential, softness, and electrophilicity index in gas phase for 4MOPIC are 5.46, -2.73, 0.183 and 0.6825 eV respectively and that of 4NPIC are 4.79, -2.40, 0.209 and 0.6013 eV respectively. Therefore, 4NPIC should be a better molecule to be involved in the interactions with electrophiles than for 4MOPIC. The dipole moment in a molecule is one of the important electronic properties when considering the interactions of molecules in solvents. The higher the value of dipole moment the stronger the intermolecular interactions would be expected, however the orientation of the dipole moment vector is also an important parameter. The calculated dipole moment values for 4MOPIC and 4NPIC in gas phase are 4.75 and 0.41 Debye respectively.

The HOMO and LUMO energies calculated in solvents revealed that both HOMOs and LUMOs experienced stabilization in 4NPIC but LUMOs are destabilized in 4MOPIC as compared to gas phase. In line with our recent report (Adeoye and Semire, 2013), the magnitude of solvation energies reflect the degree of polarity of the solvents used in these calculations (that is, Ethanol > acetone  $\approx$  DMF > THF  $\approx$  Diethyl ether). The absorption maxima calculated in solvents are shifted to longer wavelengths as compared to gas phase (Table 3). The absorption maxima calculated at DFT (B3LYP) level with 6-31G\*, 6-31G\*\*, 6-311G\*\*, 6-311+G\*\* and 6-311++G\*\* basis sets are shown in Table 4. The absorption maxima are 218.79, 218.82, 219.81, 225.53 and 225.57 nm for 4MOPIC and 276.06, 276.01, 274.52, 281.45 and 281.47 nm for 4NPIC at 6-31G\*, 6-31G\*\*, 6-311G\*\* and 6-311+G\*\* basis sets respectively. Another indicator of electrophilic attraction apart of the electrostatic potential is provided by the local ionization potential energy surface which is an overlaying of the energy of electron removal (ionization) onto the electron density. The regions with red color represent regions in the molecular surface where electron removal goes (with minimal energy) most easily, therefore easy of electron removal. The local ionization potential energy for 4MOPIC and

**Table 3.** HOMO, LUMO, energy band gap, dipole moment, solvation energy, global electrophilicity index and UV-Vis adsorption maximum calculated in gas phase and in solvents at DFT/6-31G\* level.

4MOPIC						
	G. phase	Acetone	Ethanol	Diethyl ether	DMF	THF
HOMO (eV)	-6.96	-6.79	-6.88	-6.83	-6.78	-6.81
LUMO (eV)	-1.50	-1.52	-1.61	-1.51	-1.53	-1.51
$\Delta(H-L)$	5.46	5.27	5.27	5.32	5.25	5.30
Sol. E (kJ/mol)	-43.47	-51.68	-55.54	-43.32	-51.69	-46.18
D.M	4.73	6.18	6.47	5.78	6.16	5.97
UV	218.79	219.43	219.50	219.34	219.70	217.98
H	5.46	5.27	5.27	5.32	5.25	5.30
M	-2.73	-2.69	-2.64	-2.66	-2.63	-2.65
(1/2 $\eta$ )	0.183	0.190	0.190	0.188	0.190	0.189
$\Omega$	0.6825	0.6865	0.6613	0.6650	0.6588	0.6625
4NPIC						
HOMO (eV)	-7.96	-7.70	-7.75	-7.76	-7.69	-7.73
LUMO (eV)	-3.17	-2.99	-3.11	-3.03	-2.98	-3.00
$\Delta(H-L)$	4.79	4.71	4.64	4.73	4.71	4.73
Sol. E (kJ/mol)	-32.36	-50.38	-53.94	-43.41	-50.53	-45.93
D.M	0.41	0.55	0.39	0.49	0.64	0.55
UV	276.06	288.72	295.19	285.31	288.65	286.82
H	4.79	4.71	4.64	4.73	4.71	4.73
M	-2.40	-2.36	-2.32	-2.37	-2.36	-2.37
(1/ $\eta$ )	0.209	0.212	0.216	0.211	0.212	0.212
$\Omega$	0.6013	0.5913	0.5800	0.5938	0.5913	0.5938

**Table 4.**  $\lambda_{max}$  (in nm) calculated for 4-methoxyl and 4-nitropicolinic acid at DFT with various basis sets.

DFT/	4-methoxypicolinic acid		4-nitropicolinic acid	
	UV	Intensity	UV	Intensity
6-31G*	218.79	0.16	276.06	0.035
6-31G**	218.82	0.16	276.01	0.035
6-311G**	219.81	0.16	274.52	0.038
6-311+G**	225.53	0.17	281.45	0.039
6-311++G**	225.57	0.17	281.47	0.039

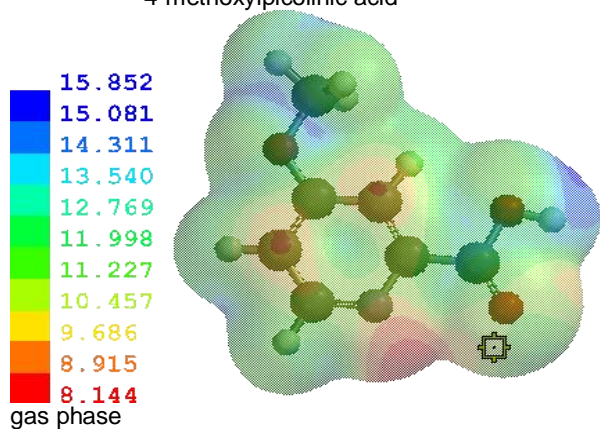
4NPIC are calculated in different solvents as displayed in Figure 3. The local ionization potential energy shows that solvents affect ionization potential of the molecules. The solvents increased the minimum energy required to remove an electron for 4MOPIC whereas the minimum energy required was lower in 4NPIC as compared to gas phase. Therefore, the minimum energy required to remove an electron in different solvents could be arranged as ethanol > acetone  $\approx$  DMF > THF > Diethyl ether > gas phase for 4MOPIC and gas phase > ethanol > diethyl ether > THF > acetone > DMF for 4NPIC. It could be suggested that increasing in electron density by electron donor substituent lowers the minimum energy required to remove an electron while decreasing in

electron density as a result of electron abstractor substituent raises the minimum energy required to remove an electron (Figure 3 and Table 5).

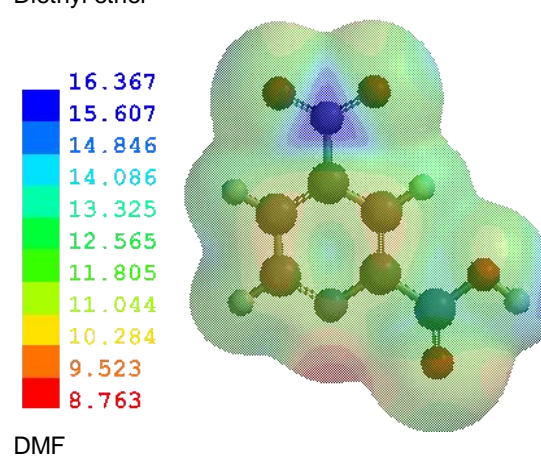
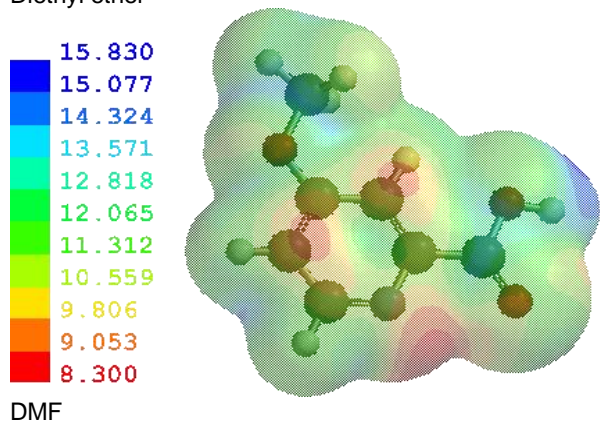
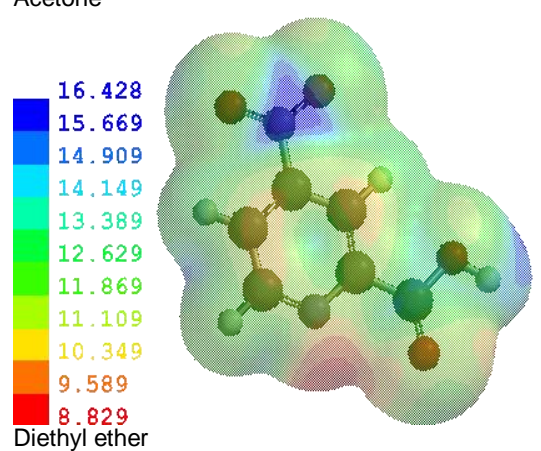
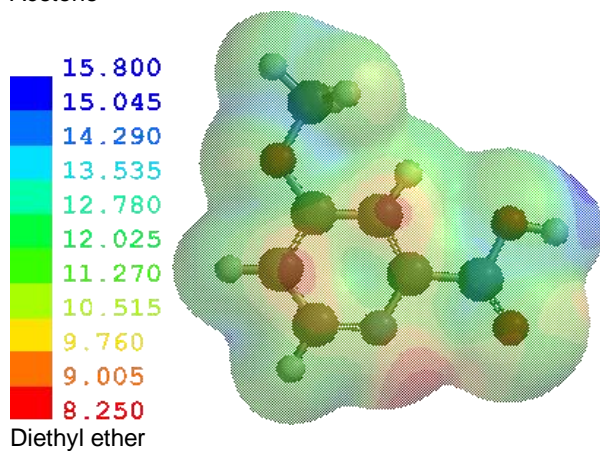
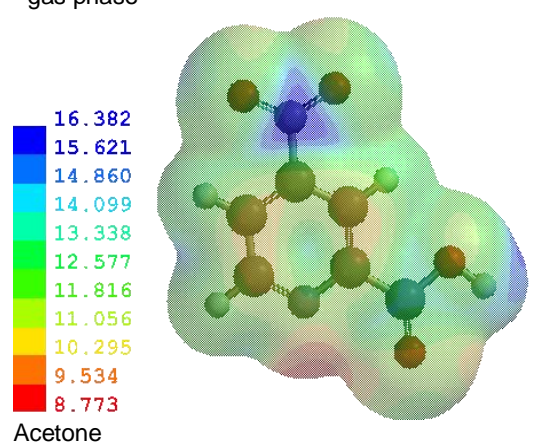
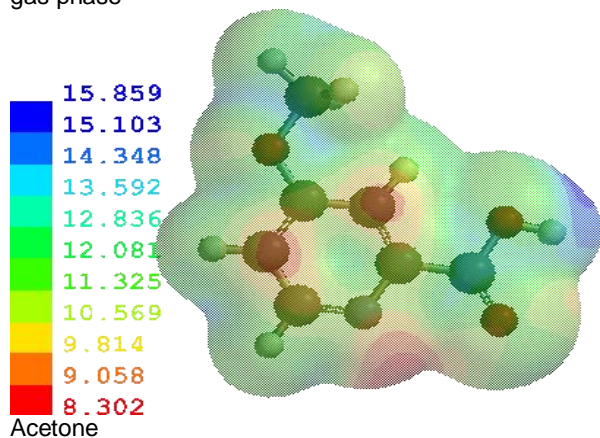
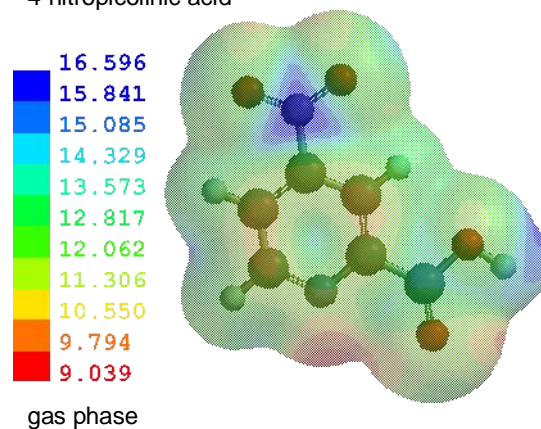
### Thermodynamic properties

The standard enthalpy ( $H^0$ ), standard entropy ( $S^0$ ) and standard heat capacity at constant pressure ( $C_p^0$ ) are 378.00, 372.77 and 138.63.94 J/mol for 4MOPIC; and 299.25, 373.34 and 136.75 J/mol for 4NPIC respectively. The thermodynamic functions such as heat capacity ( $C_{p,m}^0$ ), entropy ( $S_m^0$ ) and enthalpy ( $H_m^0$ ) for 4MOPIC and 4NPIC are obtained from the theoretical harmonic frequencies as listed in Table 5. All the  $C_{p,m}^0$ ,  $S_m^0$  and  $H_m^0$

4-methoxypicolinic acid



4-nitropicolinic acid



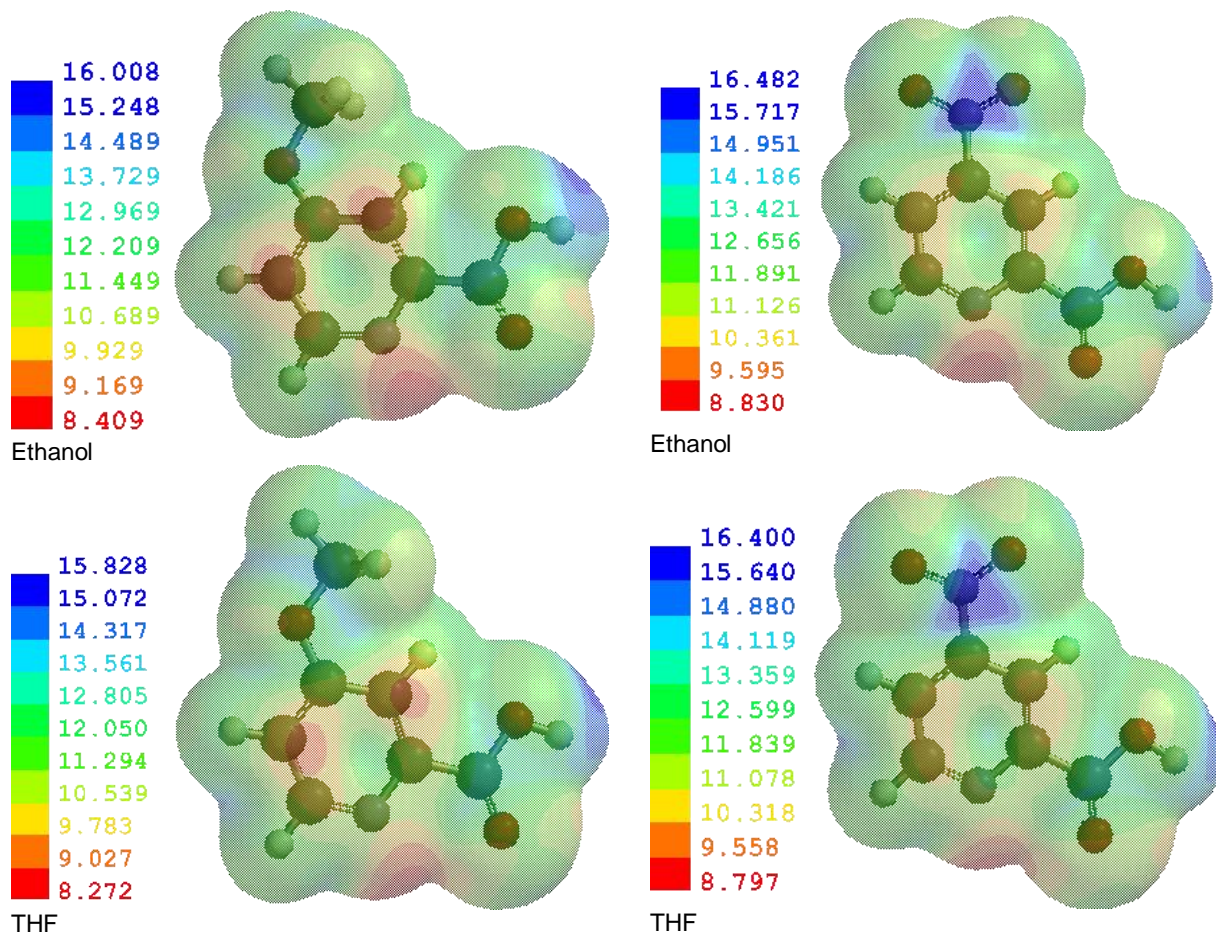


**Figure 3.** Local ionization energy surfaces on the molecular surfaces of 4MOPIC and 4NPIC with B3LYP/6-31G\*. Color ranges, in kJ/mol.

**Table 5.** The thermodynamic properties obtained at different temperature for the 4-methoxyl- and 4-nitropicolinic acid at B3LYP/6-31++G\*\* level.

Temp (K)	4MPIC			4NPIC		
	H <sup>o</sup> m (kcal/mol)	S <sup>o</sup> m (cal/mol)	Cp (cal/mol)	H <sup>o</sup> m (kcal/mol)	S <sup>o</sup> m (cal/mol)	Cp (cal/mol)
100	85.95	68.61	15.39	67.13	70.02	15.46
273	90.34	89.09	33.13	71.52	89.23	32.68
373	93.48	98.59	43.28	74.66	98.49	42.32
473	97.87	107.19	52.13	79.05	107.23	50.38
573	102.89	115.50	59.38	83.44	115.22	56.78
673	107.91	122.95	65.24	88.46	122.23	61.81
773	113.56	129.61	70.01	94.11	128.40	65.79
873	119.83	135.53	73.95	99.76	133.95	68.99
973	126.11	140.89	77.24	105.40	138.92	71.60

increases with the increase in temperature from 100 to 973K; this is due to the enhancement of molecular vibrations while temperature increases at constant pressure (1 atm). The correlations between these

thermodynamic parameters and temperature (T) are plotted and fitted by quadratic equations as shown in Figures 4, 5 and 6. The fitting factor ( $R^2$ ) for these parameters for 4MOPIC and 4NPIC is found to be 0.999

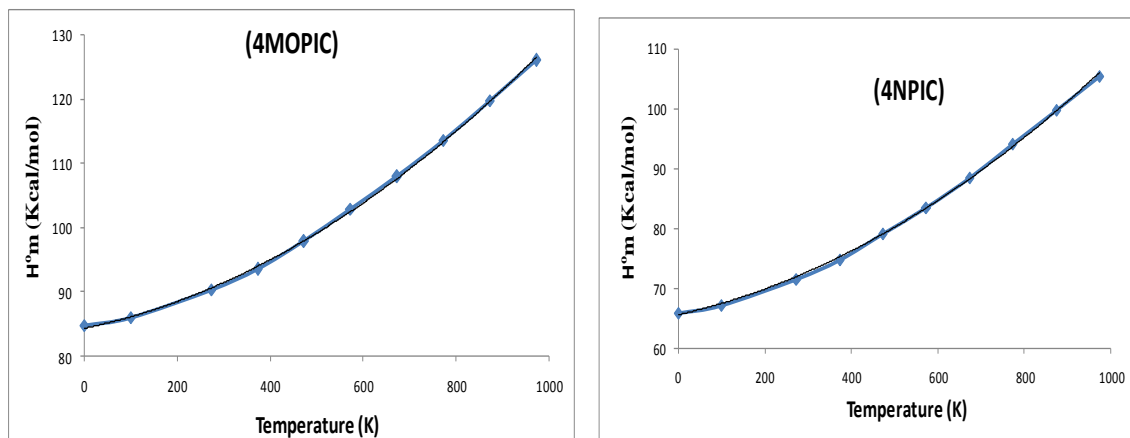


**Figure 4.** Correlation graph of enthalpy and temperature for 4-methoxypicolinic and 4-nitropicolinic.

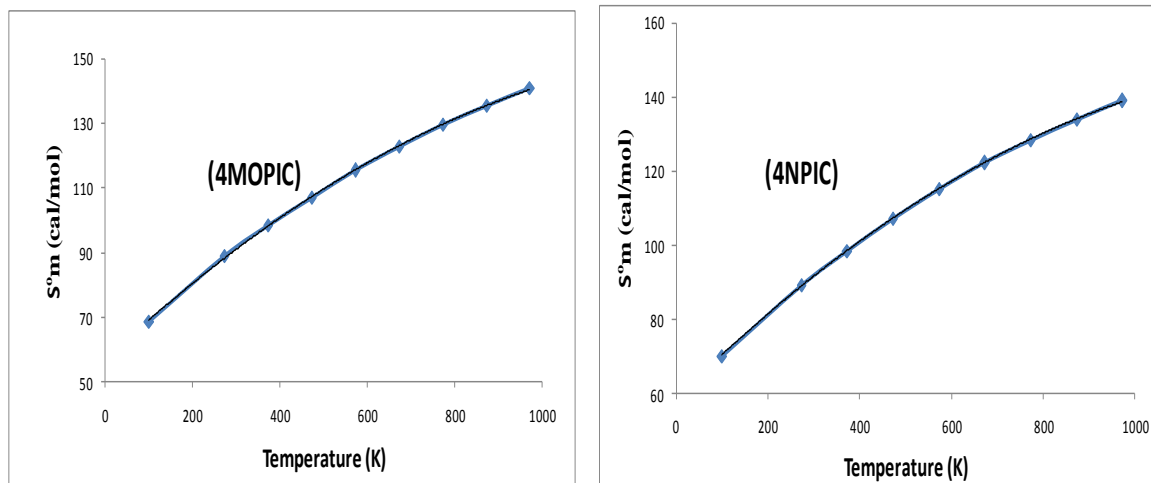


**Figure 5.** Correlation graph of entropy and temperature for 4-methoxypicolinic and 4-nitropicolinic.

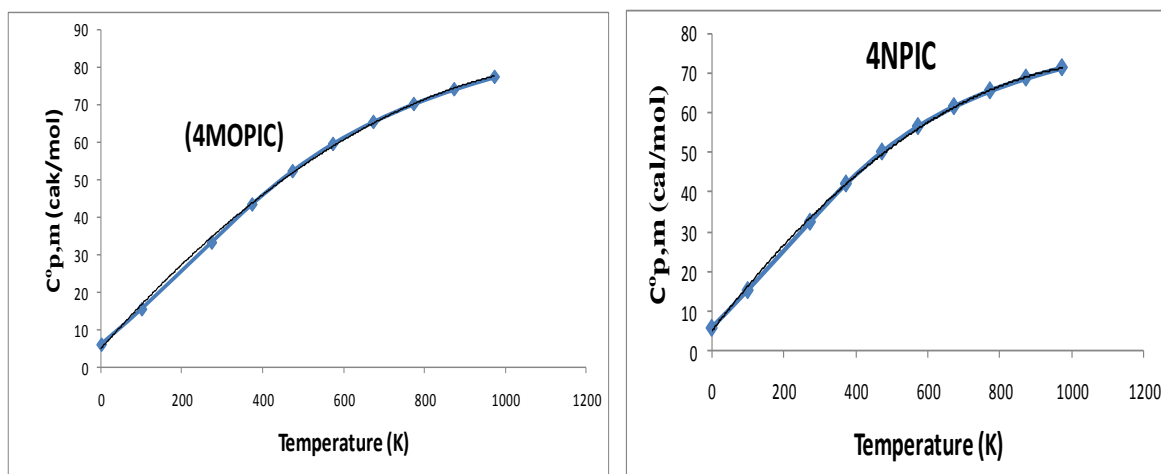


**Figure 6.** Correlation graph of heat capacity and temperature for 4-methoxypicolinic and 4-nitropicolinic.

**Table 6.** The fitting factor ( $R^2$ ) for parameters for 4MOPIC and 4NPIC.

4MOPIC	4NPIC
$C_{p,m}^0 = 4.729 + 0.121T - 5.00T^2 \times 10^{-5}$ ; ( $R^2 = 0.999$ )	$C_{p,m}^0 = 4.98 + 0.119T - 5.00T^2 \times 10^{-5}$ ; ( $R^2 = 0.999$ )
$H_m^0 = 84.32 + 0.015T + 3.00T^2 \times 10^{-5}$ ( $R^2 = 0.999$ )	$H_m^0 = 65.44 + 0.016T + 3.00T^2 \times 10^{-5}$ ( $R^2 = 0.999$ )
$S_m^0 = 56.88 + 0.126T - 4.00 \times 10^{-5}T^2$ ( $R^2 = 0.999$ )	$S_m^0 = 58.37 + 0.123T - 4.00 \times 10^{-5}T^2$ ( $R^2 = 0.999$ )

for heat capacity, enthalpy and entropy as shown in Table 6.

All the thermodynamic calculations are performed in the gas phase; therefore scale factors have been recommended for better accurate prediction (Zhang et al., 2010). All these thermodynamic data would be helpful in providing information for further study of the two isomers which can be useful to determine the directions of chemical reactions according to the second law of thermodynamics (Yazıcı et al., 2011; Nataraj et al., 2013; Govindarajanaet al., 2012).

## Conclusion

In this work, we have performed the quantum chemical calculations on geometry, vibrational frequency and electronic properties of 4MOPIC and 4NPIC using B3LYP with various basis sets. Solvents effect on the molecules are studied by using five solvents namely ethanol, acetone, diethyl ether, DMF and THF. The results show that the HOMO and LUMO energies experienced stabilization in the solvents for 4NPIC but LUMO is destabilized in 4MOPIC as compared to gas phase. The HOMO, LUMO, electrophilicity index and softness revealed that 4NPIC would be a better molecule to be involved in the interactions with electrophiles than for 4MOPIC. The absorption maxima calculated using B3LYP/6-31G\*/CIS are shifted to longer wavelengths in solvents as compared to gas phase. The minimum energy required to remove an electron in different solvents could be arranged as ethanol > acetone  $\approx$  DMF > THF > Diethyl ether > gas phase for 4MOPIC and gas phase > ethanol > diethyl ether > THF > acetone > DMF for 4NPIC.

## REFERENCES

- Adeoye IO, Semire B, (2013). Solvents effect geometries and electronic properties of picolinic acid: A theoretical study. *Int. J. Eng. Sci.* 13:101-107.
- AlHokbany N, AlJammaz I (2011). Spectroscopic investigation and density functional theory calculations of mercaptobenzothiazole and mercaptobenzimidazole ligands and their rhenium complexes. *Open J. Inorg. Chem.* 1:23-32.
- Becke AD (1988). Density-functional exchange-energy approximation with correct asymptotic behavior". *Phys. Rev. A* 38:3098-3100.
- Bird CW (1997). Heteroaromaticity. 10. The Direct Calculation of Resonance Energies of Azines and Azoles from Molecular Dimensions. *Tetrahedron.* 53:2497-2501.
- Chamizo JA, Morgado J, Sosa O (1993). Organometallic Aromaticity, *Organometallics* 12:5005-5007.
- Chattaraj PK, Maiti B, Sarkar U (2003). Philicity: A unified treatment of chemical reactivity and selectivity. *J. Phys. Chem. A* 107:4973-4975.
- Cheeseman JR, Trucks GW, Keith TA, Frisch MJ, (1996) A comparison of models for calculating nuclear magnetic resonance shielding tensors", *J. Chem. Phys.* 104:5497-5509.
- De Proft F, Geerlings P (2001). Conceptual and computational DFT in the study of aromaticity. *Chem. Rev.* 101:1451-1464.
- Dimitrijević DM, Tadić ŽD, Mišić-Vuković MM, Muškatriović M (1974). Investigation of electronic effects in the reaction of diazodiphenylmethane with pyridine and pyridine N-oxide carboxylic acids, *J. Chem. Soc. Perkin Trans.* 2:1051-1055.
- Domingo LR, Aurell M, Contreras M, Perez P (2002). Quantitative Characterization of the Local Electrophilicity of Organic Molecules. Understanding the Regioselectivity on Diels-Alder Reactions. *J. Phys. Chem. A.* 106:6871-6876.
- Drmanic SZ, Nikolic JB, Marinkovic AD, Jovanovic BZ (2012). A comparative study of the linear solvation energy relationship for the reactivity of pyridine carboxylic acids with diazodiphenylmethane in protic and aprotic solvents. *J. Serb. Chem. Soc.* 77:1311-1338.
- Evan GW, Johnson PE (1980). Characterization and quantitation of a zinc binding ligand in human milk. *Peiatr. Res.* 14:876-880.
- Fernandez-Poi JA, Hamilton PD, Klos DJ (2001). Essential viral and cellular zinc and iron containing metalloproteins as targets for prevention and therapy of viral diseases and cancer. *Anticancer Res.* 21:931-56.
- Gfeller M, Furrer G, Schullin R (1976). Use of completely mixed flow-through systems: hydrolysis of phenyl picolinate. *Environ. Sci. Technol.* 31:3692-3701.
- Goher MAS, Abu-Youssef MAM (1996). Synthesis, Spectral and Structural Characterization of a Monomeric Chloro Complex of Zinc(II) with Picolinic Acid;  $[Zn(C_5H_4NCO_2H)(C_5H_4NCO_2)Cl]$ . *Polyhedron* 15:453-457.
- Govindarajana M, Karabacak M, Periandy S, Tanuja D (2012). Spectroscopic (FT-IR, FT-Raman, UV and NMR) investigation and NLO, HOMO-LUMO, NBO analysis of organic 2,4,5-trichloroaniline. *Spectrochim Acta. A.* 97:321-245.
- Kalinowska M, Borawska M, Swislocka R, Piekut J, Lewandowski W (2007). Spectroscopic (IR, Raman, UV,  $^1H$  and  $^{13}C$  NMR) and microbiological studies of Fe(III), Ni(II), Cu(II), Zn(II) and Ag(I) picolines. *J. Mol. Struct.* 834-836:419-415.
- Kalinowski HO, Berger S, Braun S (1988). Carbon-13 NMR spectroscopy, John Wiley and Sons, Chichester.
- Karakurt T, Dinçer M, Çukurovalı A, Yılmaz I (2012). Ab initio and semi-empirical computational studies on 5-hydroxy-5,6-di-pyridin-2-yl-4,5-dihydro-2H-[1,2,4]triazine-3-thione *J. Mol. Struct.* 1024:176-188.
- Koczon P, Dobrowolskic J.Cz, Lewandowski W, Mazurek AP (2003). Experimental and theoretical IR and Raman spectra of picolinic, nicotinic and isonicotinic acids. *J. Mol. Struct.* 655:89-95.
- Koopmans T (1734). Ordering of wave functions and eigenvalues to the individual electrons of an atom, *Physica.* 1:104-113.
- Kukovec BM, Popovic Z, Komorsky-Lovric Š, Vojkovic V, Vinkovic M (2009). Synthesis, structural, spectroscopic and thermal characterization of cobalt complexes with 3- and 6-methylpicolinic acid. Voltammetric and spectrophotometric study in solution *Inorganica Chimica Acta* 362:2704-2714.
- Lee CT, Yang WT, Parr RG (1988). Development of the Colle-Salvetti correlation-energy formula into a functional of the electron density, *Parr, Phys. Rev. B* 37:785-589.

- Marinkovi AD (2005). Investigations of the reactivity of pyridine carboxylic acids with diazodiphenylmethane in protic and aprotic solvents. Part I. Pyridine mono-carboxylic acids. *J. Serb. Chem. Soc.* 70:557–567.
- Nataraj A, Balachandran V, Karthick T (2013). Molecular orbital studies (hardness, chemical potential, electrophilicity, and first electron excitation), vibrational investigation and theoretical NBO analysis of 2-hydroxy-5-bromobenzaldehyde by density functional method. *J. Mol. Struct.* 2031:221-233.
- Parajón-Costa BS, Wagner CC, Baran EJ (2004). Vibrational spectra and electrochemical behavior of Bispicolinate copper(II). *J. Argentine Chem. Soc.* 92:109-117.
- Parr RG, Szentpaly L, Liu S (1999). Electrophilicity Index, *J. Am. Chem. Soc.* 121:1922-1924.
- Pearson RG (1993). The principle of maximum hardness, *Acc. Chem. Res.* 26:250-255.
- Pihlaja K, Kleinpeter E (1994). Carbon-13 Chemical Shifts in Structural and Stereo Chemical Analysis, VCH Publishers, Deerfield Beach.
- Semire B (2013). Density Functional Theory studies on electronic properties of thiophene S-oxides as aromatic dienophiles for reactivity prediction in Diels-Alder reactions. *Pakistan J. Sci. Ind. Res. A* 56:14-18.
- Semire B, Odunola OA (2013). Theoretical Study on nucleophilic behaviour of 3,4-Dioxa-7-thia-cyclopenta[a]pentalene and 3,7-Dioxa-4-thia-cyclopenta[a]pentalene using ab initio and DFT based reactivity descriptors. *Int. J. Chem. Mod.* 4:87-96.
- Stare J, Jezierska A, Ambrožič G, Košir IJ, Kidrič J, Koll A, Mavri J, Hadž D (2004). Density Functional Calculation of the 2D Potential Surface and Deuterium Isotope Effect on <sup>13</sup>C Chemical Shifts in Picolinic Acid N-Oxide. Comparison with Experiment. *J. Am. Chem. Soc.* 126:4437.
- Takusagawwa F, Shimada A (1976). Isonicotinic Acid. *Acta Cryst B* 32:1925-1927.
- Teimouri A, Chermahini AN, Emami M (2008). Synthesis, characterization, and DFT studies of a novel azo dye derived from racemic or optically active binaphthol. *Tetrahedron* 64:11776–11782.
- Varsanyi G, Sohar P (1972). Infrared spectra of 1,2,3,5-tetra-substituted benzene derivatives. *Acta Chim. Acad. Sci. Hung.* 74:315-333.
- Yazıcı S, Albayrak C, Gümrükçüoğlu I, Senel I, Büyükgüngör O (2011). Experimental and density functional theory (DFT) studies on (E)-2-Acetyl-4-(4-nitrophenyldiazenyl) phenol. *J. Mol. Struct.* 985:292-298.
- Yurovskaya MA, Mitkin OD, Zaitsera FV (1998). Functionalization of pyridines 2. Synthesis of Acylpyridines, pyridinecarboxylic acids and their derivatives. *Review Chemistry of Heterocyclic compounds* 34:871- 879.
- Zhang R, Dub B, Sun G, Sun Y (2010). Experimental and theoretical studies on o-, m- and p-chlorobenzylideneaminoantipyrines. *Spectrochim Acta*, 75A:1115-1124.
- Zhou Z, Navangul HV (1990). Absolute hardness and aromaticity: MNDO study of benzenoid hydrocarbons, *J. Phys. Org. Chem.* 3:784-788.
- Ziegler T (1991) Approximate density functional theory as a practical tool in molecular energetic and dynamics. *Chem. Rev.* 91:651-667.

*Full Length Research Paper*

## Neuro-fuzzy decision learning on supply chain configuration

J. C. Garcia Infante<sup>1</sup>, J. J. Medel Juarez<sup>2</sup> and J. C. Sanchez Garcia<sup>1\*</sup>

<sup>1</sup>Mechanical and Electrical Engineering School IPN, Col. San Francisco Culhuacan Del. Coyoacán, D. F. ext.73092 Mexico.

<sup>2</sup>Computing Research Centre, Av. 100 m, esq., Venus, Col. Nueva Industrial Vallejo, C. P. 07738 D. F. ext. 56570 Mexico.

Accepted 1 July, 2013

**This paper describes the computational automatic supply chain configuration (SCC) based on fuzzy logic prediction actualizing automatically the chain stages considering different customer service level petitions. Each level is selected in accordance with the inference and the knowledge base process supplies (KBPS). The SCC model as an intelligent processes selector (IPS), allows dynamical configuration in accordance with the minimum cost supplies configuration (MCSC) described with the SCC functional error. The basic future decisions set as a knowledge base (KB) using fuzzy rules and inferences, transforms the proposed decisions into actions over the elements required by the process supply (PS). The minimal functional error and the SCC best selection, permits excellent client attention. The adaptive model stages operational SCC is described illustratively using Matlab<sup>®</sup> software.**

**Key words:** Fuzzy digital learning, neural networks, supply chain configuration.

### INTRODUCTION

Intelligent supply chain (ISC) structure is built dynamically considering the competitive actions inside the dynamical world, where customers have different services and product requirements. The enterprises should have new approaches that can help to support customer innovation, flexibility, quality, and excellent service maintenance to increase their competence. The multiple scenarios analysis allows developing the strategies for the supply chain configuration (SCC), considering different customer service levels increasing the decision-making support affecting global efficiency (Croom et al., 2000). ISC viewed as an intelligent process requires a mechanism that deduces previously the customer wishes (requirements or specifications) described dynamically as a class of service (CS). In agreement to CS degree the ISC transforms the service into a specific grade, according to the structure conditions with minimum cost

and customer requirements. Therefore, the ISC selected the best attention level answer. An intelligent structure has different supply scenarios with different interpretations, considering the actual customer requirements, having automatic SC changing stage process (Chong and David, 2011). The customer requirements prediction is based on a fuzzy learning system that adjusts dynamically the process stage conditions through the parametre weights with respect to the mean square error criterion or functional error.

The learning system scheme inferences and the knowledge base process is the tool considered as the ISC in accordance with different types of service changes. The learning technique selects the best service for each requirement and obtains the knowledge. Concerning the enterprise processes, the fuzzy intelligent tools viewed as a learning system is an option to obtain

\*Corresponding author. E-mail: [jcnet21@yahoo.com](mailto:jcnet21@yahoo.com)

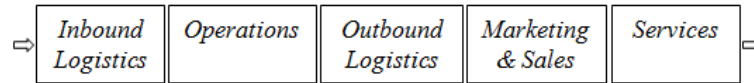


Figure 1. The supply chain stages.

different types of service, dynamically interacting with the customer needs, having an adaptation of the ISC answer in accordance to the possible changes. The customer attention uses a rule set based on the Takagi and Sugeno (TS) mechanism which requires a feedback law, adjusting the process parameters, minimizing the functional error response to updating the process (García et al., 2011).

With this perspective, this paper introduces the Fuzzy learning system (FDF) analyzing and improving the supply chain configuration structure, giving answers levels with respect to the customer requirements, changing the enterprise structure in a natural sense. This selects a specific decision using an ISC configuration in order to give the best service level to each possible scenario. In a novel view, this provides a roadmap improving the enterprise, having a different configuration level support for the supply chain (Korena and Shpitalni, 2010).

### SC configuration description

A supply chain integrates a set of links that makes up an economic process from the supplier to the distribution of finished products. Each stage process has to add value as a goal. Each individual stage should be reviewed in order to obtain the best service response. In accordance with the type of service required by the customer and the best response levels at each stage, integrating and optimizing the supply chain for the enterprise structure gives the best service response to the customer. Figure 1 shows the SC in general form (Croom et al., 2000). The SC structure integrates the next stages, as seen in Figure 1:

Inbound logistics: receiving, storing, inventory, control and transportation scheduling.

Operations: machining, packaging, assembly, equipment maintenance, testing.

Outbound logistics: warehousing, order fulfillment, transportation, distribution.

Marketing and sales: channel selection, advertising, promotion, selling, pricing, retailing.

Services: support, repair, installation, training, parts management.

There are different ways to develop a supply chain as an automated intelligent process in order to optimize the enterprise services and make better decisions. Most used is expertise and heuristics. This case used a learning

system integrating all the possible SC configurations to an enterprise structure inferring the type of service needed and dynamically selecting the best SC configuration giving the best customer level answer (Craves and Tomlin, 2003; Korena and Shpitalni, 2010). Each stage is analyzed separately, generating more value to the chain. To decide how to configure the SC needs to consider some characteristics that could be changed in order to obtain the best service level required by the customer, for example, the product type, velocity, category, demand, cost, suppliers and other attributes. The best configuration solution is usually defined as minimizing or maximizing a specific variable at each SC stage (Giunipero et al., 2008).

If an enterprise needs different service levels with a specific type of service required by the customer an intelligent process has to change to customer specifications. It needs to have different specific SC configurations optimizing the service level. The SC will always keep the same stages, but each of these stages will modify its value to configure the SC to a new service level for the customer needs and the enterprise type of service selected with minimum cost. The following stages allow specific service level in accordance with the SC selected (Chong and David, 2011; Yao, 2010):

- (i) The customer invokes a specific type of service required
- (ii) The learning process infers the actual customer needs
- (iii) The selection stage gets the best supply chain configuration
- (iv) The process has an update in order to give the corresponding service level

### LEARNING SYSTEM DESCRIPTION

The learning system structure has an intelligent structure that infers a real process change with an actual situation. This improves a dynamical process operation because the learning description will give the best answer condition to update the process configuration and work with the optimal operation level in accordance with the changes. The objective of the learning system is the parameter estimation described as  $\hat{a}_k$ . When the customer selects a specific type of service described as  $t_k$  the enterprise offers the learning system that will obtain the specific parameters sequence of  $\hat{a}_k$  to update the learning mechanism. This approximation to the

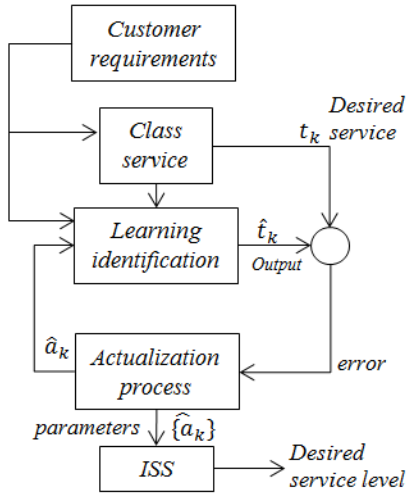


**Figure 2.** Identification structure services SC model.

desired type of service describes the actual customer requirements automatically (García et al., 2011; Mamdani, 1974).

The learning system has a structure that classifies its answers with different operational levels in order to select the corresponding parametre  $\hat{a}_k$  from a knowledge base (KB), using the logic connectors *if-then*, to update the learning system weights describing the actual desired type of service. The next stage called intelligent supply selection (ISS), infers the  $\hat{a}_k$  sequence selecting the best SC configuration values with the best service level (Craves and Tomlin, 2003; Zadeh, 1965). Figure 2 shows the learning system operation structure (García et al., 2011; Korena and Shpitalni, 2010; Takagi and Sugeno, 1986).

Figure 2 describes the learning system operation, where  $t_k$  represents the actual desired type of service,  $\hat{t}_k$  as the signal approximation of the actual service type,  $e_k$  is the error between both signals and  $\{\hat{a}_k\}$  is the estimated parametres sequence by the learning process representing a specific value sequence identifying the respective type of service. The selection process stage will use the parametres value  $\{\hat{a}_k\}$  as a learning process inferring the type of service and selecting the best SC service level (Passino, 1998).

The FLP has a knowledge base, which is limited by the mean square error described in Equation (1). The knowledge base has all the possible values of  $\hat{a}_k$  corresponding with the desired input system service. These membership values of  $\hat{a}_k$  are selected by a process dynamically update its weights, with the service changes type  $t_k$  and the criterion minimizing the

estimation error obtaining the best approximation of the learning output system  $\hat{t}_k$  (Mamdani, 1974).

$$k \langle J_k, J_k^T \rangle = \left[ \langle \Delta_k, \Delta_k^T \rangle + (k-1) \langle J_{k-1}, J_{k-1}^T \rangle \right] \in \mathfrak{R}_{[0,1]}^+ \quad (1)$$

**Theorem**

Let the learning system description in Equation (2)

$$t_k = a t_{k-1} + w_k \quad (2)$$

Where  $t_k \in \mathfrak{R}^+$  as the service changes type,  $a \in \mathfrak{R}_{[-1,1]}$  as a specific service parametre and,  $w_k$  as the actual situation; has an optimal estimation Equation (3).

$$\hat{a}_k \rightarrow a + \varepsilon_k \quad (3)$$

**Proof**

In agreement to  $\Delta_k = t_k - \hat{t}_k$ , the quadratic form  $\Delta_k^2$  into functional error (1) with Equation (2), has Equation (4).

$$k \langle J_k, J_k^T \rangle = a^2 \langle t_{k-1}, t_{k-1}^T \rangle + \langle w_k, w_k^T \rangle - \langle \hat{t}_k, \hat{t}_k^T \rangle + 2a \langle t_{k-1}, w_k^T \rangle - 2a \langle t_{k-1}, \hat{t}_k^T \rangle - 2 \langle w_k, \hat{t}_k^T \rangle + (k-1) \langle J_{k-1}, J_{k-1}^T \rangle \quad (4)$$

In Equation (4) the stochastic gradient with respect to "a" obtaining Equation (5).

$$a = \frac{\langle t_{k-1}, \hat{t}_k^T \rangle - \langle t_{k-1}, w_k^T \rangle}{\langle t_{k-1}, t_{k-1}^T \rangle} \quad (5)$$

Where, the paramtre and perturbation are described respectively in Equation (5).

$$\hat{a}_k \cong \frac{\langle t_{k-1}, \hat{t}_k \rangle}{\langle t_{k-1}, t_{k-1}^T \rangle}, \quad \varepsilon_k \cong - \frac{\langle t_{k-1}, w_k^T \rangle}{\langle t_{k-1}, t_{k-1}^T \rangle} \quad (6)$$

Finally, the estimator is optimal and has the form (3). Then the convergence exists when  $\langle t_{k-1}, w_k \rangle \rightarrow 0$  ■.

Where "a", represents the reference variable obtaining a specific service parametre; "m" is the number of

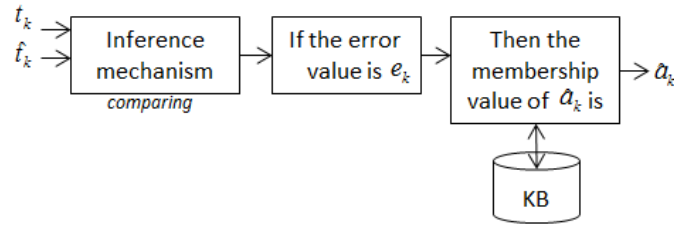


Figure 3. Fuzzy Inference Mechanism based on error values.

elements of each type of service, representing the SC stages number and; " $\varepsilon_k$ " represents the region where the results are considered acceptable.

The functional error when  $k \rightarrow m$ , converge to  $\delta_m$ , where  $k \langle \delta_m, \delta_m \rangle = \sum_{i=1}^m (\varepsilon_i, \varepsilon_i^T)$  and in recursive form  $= \langle \varepsilon_m, \varepsilon_m^T \rangle + (m-1) \langle \delta_{m-1}, \delta_{m-1} \rangle$ .

For dynamic parameters selection, in accordance with the description of the actual type of service  $t_k$  and the FLP  $\hat{t}_k$ , have the best signal approximation. This is an indicator process with respect to the actual type of service parameters. The different operational levels inside the FLP must accomplish the error criterion described in Equation (1) (García et al., 2011).

To extract the learning identification parameters in fuzzy form uses the mechanism shown in Figure 3, and uses the logic connectors *if-then*, based on a TS inference dynamically, selecting the best parameters value to the internal FLP classification levels. The different type of services, use the knowledge base that has the membership values of  $\hat{a}_k$ .

The fuzzy process with respect to the criterion described as  $\lim_{k \rightarrow m} J_k \rightarrow J_{\min}$ , makes a selection of the

knowledge base parameters, permitting an approximation of the output signal  $\hat{t}_k$ , to each actual desired service described as  $t_k$ . The learning system selection process is in heuristic form, based on probabilistic properties system. This establishes the operational levels bounded by the error functional as:  $J_k \subseteq [\delta_{\min}, \delta_{\max}]$ . To each level,

the process selects a specific value of  $\hat{a}_k$ , having as a goal the best approximation of  $\hat{t}_k \cong t_k$  (Craves and Tomlin, 2003; Takagi and Sugeno, 1986).

For parameter selection of the KB into the FLP, it is important for the functional error value to take a parameter value from the knowledge base, when the functional error obtains its minimum value, approximating  $\hat{t}_k$  to  $t_k$ , and is the smallest distance between both

values. To each operation level the learning approach has a specific parameter configuration value updating the process mechanism. The goal is obtaining the minimum error difference approximation between the type of service required by the customer and the learning identification deducing the SC specific service level configuration (Korena and Shpitalni, 2010).

**ISC selection process**

The learning system architecture integrates a stage process selection that uses the parameters obtained from the previous learning stage described as  $\{\hat{a}_k\}$  to each type of service level. This stage operates as a neural net that deduces the best SC configuration in accordance to the actual type of service. First, training the knowledge base network (KBN), the learning system gets the representative parameter sequences to each level previously at the training stage (implementation). It selects the value sequence to each type of service in  $\{a_{kBn}\}$ . All the possible

$\{a_{KBn}\}$  describes different levels stored in the KBN of the Neural Net. This makes a classification of the different SC service levels with the possible type of service to be selected by the customer (Chong and David, 2011; Marcek, 2004).

This stage selection makes a comparison between the actual learning identification parameters  $\{\hat{a}_k\}$  and each sequence  $\{a_{kBn}\}$  stored previously in the knowledge base network obtaining the error value. The error rank establishes the correspondence to SC configuration using fuzzy rules which recognize and select the configuration service type. The TS inference has the sequence described as  $[\{\hat{a}_k\}, \{a_{kBn}\}]$ . Figure 4, shows the network structure to select the SC configuration (Marcek, 2004).

The neural architecture represents the stages, which obtain the parameter information described as  $\{\hat{a}_k\}$  in the learning system. This process starts with first layer (input) and continues to the other neurons, in the hidden layer. The neuronal structure process from the previous nodes allows the following stages, having as a goal identifying the corresponding SC configuration (Marcek, 2004):

(i) Inference layer: The error criterion service level described as  $D_e$ , into the rank  $[0, \varepsilon_k]$ ,  $\varepsilon_k \in \mathfrak{R}^+$ , makes a comparison of actual  $\{\hat{a}_k\}$  and the  $\{a_{kBn}\}$  stored in the knowledge base. The minimum error distance between values considers the rank error

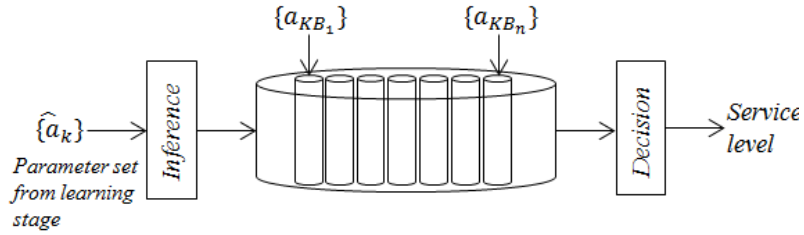


Figure 4. Supply chain configuration selection.

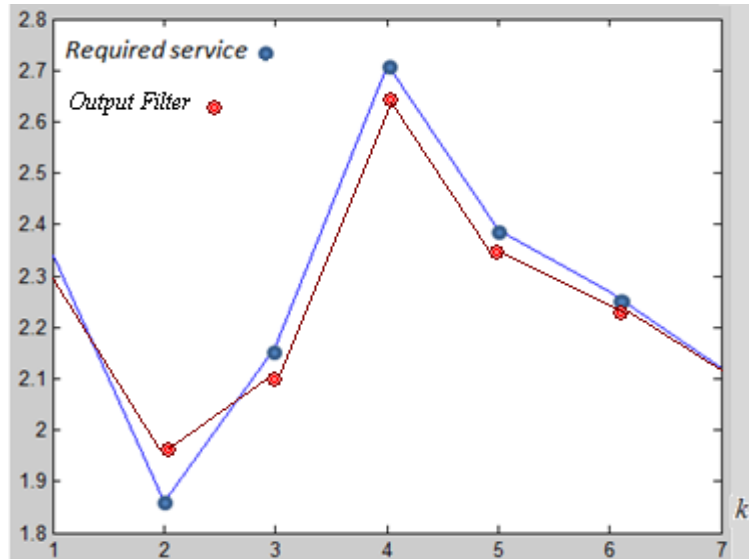


Figure 5. Learning stage applied into identification parameters.

defined previously (García et al., 2011). The error is described by the distance between the  $\{\hat{a}_k\}$  as actual parameters value and the stored sample  $\{a_{kBn}\}$ , given that

$d(\{\hat{a}_k\}, \{a_{ID}\}) \in \{D_a\} \{D_a\} \subset R^+_{[0, \epsilon_k]}$ , then  $\{\hat{a}_k\}$  has a membership function into the knowledge base neural net corresponding to SC configuration. However, in the case of  $d(\{\hat{a}_k\}, \{a_{ID}\}) \notin \{D_a\}$ , then  $\{\hat{a}_k\}$  does not belongs to the network, then there is no type of service required by the customer and it cannot select a corresponding SC configuration.

(ii)Actualization layer: This stage makes the update of the SC configuration value to the service level required for the process in accordance with the actual type of service selected by the customer, using a set of fuzzy rules (if-then) to this inference process (Korena and Shpitalni, 2010). If the  $\{a_{kBn}\}$  set value from the Bn is the service level 1, then the SC configuration is selected.

**SIMULATION**

For simulation there are five possible supply chain options to choose in order to satisfy customer needs with

the minimum cost. First, the customer configures their requirements in the database, and the learning identification stage obtains the parameters that corresponds to customer needs. The network gets the parameters and makes a selection of the best corresponding supply chain configuration complying with customer selection with minimum cost for the business, which provides a dynamic decision making different possible service levels (García et al., 2011; Zadeh, 1965). Figure 5, shows the learning approximation requirements in order to obtain the parameters to be used in the selection stage. Figure 6, is the learning stage convergence (1) based on the mean square error in accordance with the approximations. In the selection process, the network has an inference stage that compares the learning stage parameter values with the values stored into the knowledge base. This comparison process is shown in Figure 7.

Figure 8, shows the possible supply chains configurations stored at the knowledge base. It could have more configurations stored, considering the capacity and flexibility of the company. In accordance with customer needs and the error distance of Figure 7,

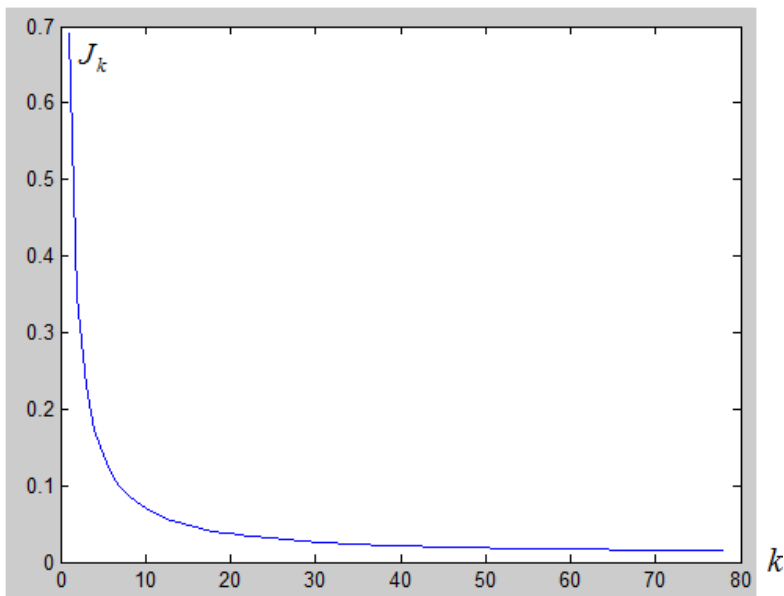


Figure 6. Recursive stage error.

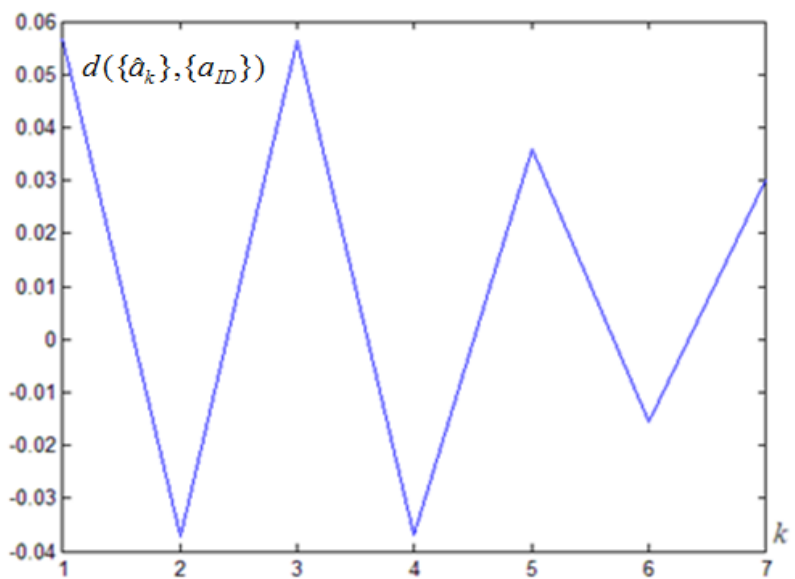


Figure 7. Error inference at the network stage.

one supply configuration will be selected. The service level represents the supply chain selected in the process. Figure 9 shows the configuration with the minimum cost, considering the best service for customer requirements.

**CONCLUSIONS**

The supply chain in the learning system needs a Neuro-

fuzzy model with dynamical decisions offering to the customer different possible service levels. In this paper customer service was viewed with the decisions selected in an intelligent form, estimating the best coefficients required by the supply process. The decisions were defined in the knowledge base using inferences rules and transformed into actions required for the supply process. Automatically, all the supply structure was adjusted in accordance with customer needs and minimum cost. The

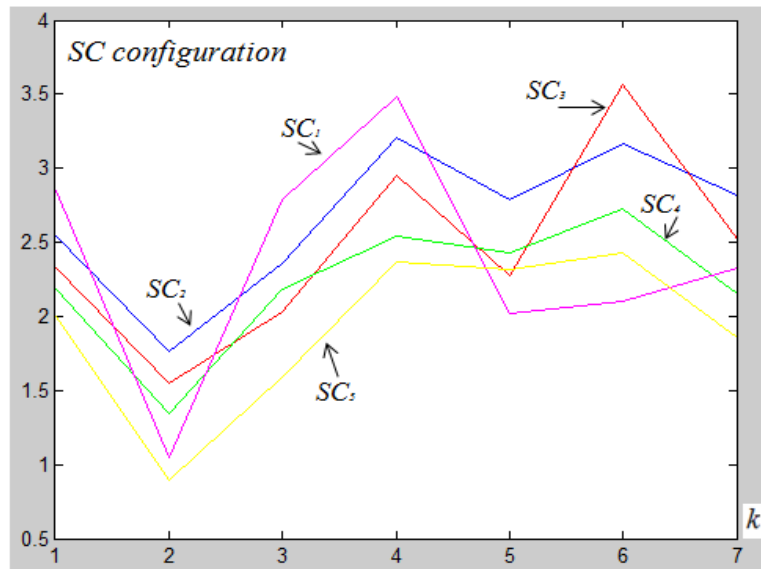


Figure 8. Supply chain set to be selected in the network.

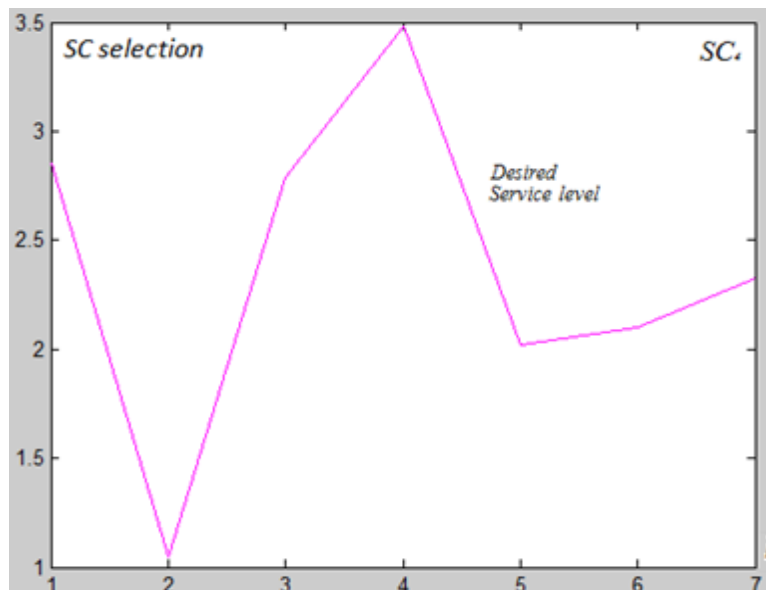


Figure 9. Supply chain selected with the minimum cost as a service level.

simulation of this process shows the operation of the dynamic supply chain using a learning process that describes customer requirements obtaining the parameters, and then the supply chain selection process with a neural network structure.

REFERENCES

Chong W, David B (2011). A literature review of decision-making models and approaches for partner selection in agile supply chains. *J. Purchasing Supply Manage.* 17(4):256–274.

Craves SC, Tomlin BT (2003). Process Flexibility in Supply Chains, *Manage. Sci.* 49(7):907–919.  
 Croom S, Romano P, Giannakis M (2000). Supply chain management: an analytical framework for critical literature review, *Eur. J. Purchasing Supply Manage.* 6:67-83.  
 García JC, Medel JJ, Sánchez JC (2011). Filtrado digital neuronal difuso: caso MIMO, *Revista Ingeniería e Investigación*, 31(1):184-192.  
 Giunipero LC, Hooker RE, Joseph-Matthews S (2008). A Decade of SCM Literature: Past, Present and Future Implications. *J. Supply Chain Manage* 44(4):66-86.  
 Korena Y, Shpitalni M (2010). Design of reconfigurable manufacturing systems, *J. Manufacturing Syst.* 29:130–141.  
 Mamdani E (1974). Applications of Fuzzy Algorithms for Control of

- Simple Dynamic Plant. Proc. IEEE, 121:1585-1588.
- Marcek D (2004). Stock Price Forecasting: Statistical, Classical and Fuzzy Neural Networks., Modeling Decisions for Artificial Intelligence, Springer Verlag, pp. 41-48.
- Passino KM (1998). Fuzzy Control, USA, Addison Wesley.
- Takagi T, Sugeno M (1986). Fuzzy Identification of Systems and its Applications to Modelling and control. IEEE Trans. Syst. Man. cybernetics, 15:116-132.
- Yao J (2010). Decision optimization analysis on supply chain resource integration in fourth party logistics, J. Manufacturing Syst. 29:121–129.
- Zadeh L (1965). Fuzzy Sets. Information and control, 8:338-353.

*Full Length Research Paper*

## Simulation and analysis: The effect of mobility on IPTV (VOD) over wi-max using OPNET

Gurmeet Singh and Amit Grover\*

Department of Electronics and Communication Engineering, Shaheed Bhagat Singh State Technical Campus, Moga road, Ferozepur-152004, Punjab, India.

Accepted 1 July, 2013

**In this paper, the effect of mobility of mobile Wi-max subscribers on video on demand (VOD) over Wi-max is analysed by considering the scalable video coding (SVC) codes for video streaming. This experiment has been carried out using OPNET modeller 14.5. To compare the performance of Internet Protocol television (IPTV) over Wi-max, the packet delay variation, packet end to end delay, delay and load matrices are used. The result shows that after certain speed, the load increases, the delay again decreases and there is no change in the packet delay variation and packet end to end delay.**

**Key words:** Wi-max, OPNET, scalable video coding (SVC), wireless networks, IEEE 802.16, internet protocol television (IPTV).

### INTRODUCTION

At present, wireless technology has become the most exciting at our surrounding environment; many types of techniques are used to make a communication through wireless network like MANET, VANET, Wi-Fi, bluetooth, Wi-max etc. As per increasing popularity of broadband internet wireless networking (OPNET official website, <http://www.opnet.com>; Eklund et al (2006). Wi-max have used in the field of wireless technology. Wi-max is wireless interoperability for microwave access. It is the latest technology for wireless communication which is based on the IEEE 802.16-2004 and IEEE 802.16e-2005 standards and was designed with much influence from Wi-Fi (Daniel, 2004; Easwarakumar and Parvathi, 2012) IEEE 802.16 supports two types of transmission duplexing: Time division duplexing (TDD) and frequency division duplexing (FDD) and support both full and half duplex stations (Aamir et al., 2009; Shraddha and Upadhyay, 2009; Rakesh et al., 2011). Wi-max is illustrating the principles of orthogonal frequency division multiplexing (OFDM) which is a suitable modulation/access technique for non-line-of-sight (LOS) conditions

with high data rates. The IEEE 802.16 suite of standards (IEEE 802.16-2004/IEEE 802.16e-2005) (Saul et al., 2010; Aamir et al., 2009) defines within its scope four PHY layers, any of which can be used with the media access control (MAC) layer to develop a broadband wireless system (Daniel, 2004; Schwarz et al., 2007). The PHY layers defined in IEEE 802.16 (Eklund et al., 2006; Mai et al., 2008) are:

- (i) Wireless MAN SC, a single-carrier PHY layer intended for frequencies beyond 11GHz requiring a LOS condition. This PHY layer is part of the original 802.16 specifications.
- (ii) Wireless MAN SCa, a single-carrier PHY for frequencies between 2GHz and 11GHz for point-to-multipoint operations.
- (iii) Wireless MAN OFDM, a 256-point FFT-based OFDM PHY layer for point-to-multipoint operations in non-LOS conditions at frequencies between 2GHz and 11GHz. This PHY layer, finalized in the IEEE 802.16-2004 specifications, has been accepted by Wi-max for fixed

\*Corresponding author. E-mail: [amitgrover\\_321@rediffmail.com](mailto:amitgrover_321@rediffmail.com).

operations and is often referred to as fixed Wi-max.

(iv) Wireless MAN OFDMA, a 2,048-point FFT-based OFDMA PHY for point-to-multipoint operations in NLOS conditions at frequencies between 2GHz and 11GHz.

The main purpose of IEEE 802.16 technology was to provide last-mile broadband wireless access as an alternative to cable, digital subscriber line service. In Wi-max the communications is done in two ways that is, management message and data messages. Management messages are used to govern communications parameters necessary to maintain wireless links, and data messages carry the data to be transmitted over wireless links.

## FUNDAMENTAL WIMAX CONCEPTS

Wi-max networks have five fundamental architectural components (Aamir et al., 2009; Rakesh, 2011; Cicconetti et al., 2007):

### Base station (BS)

The BS is the node that logically connects wireless subscriber devices to operator networks. The BS maintains communications with subscriber devices and governs access to the operator networks. A BS consists of the infrastructure elements necessary to enable wireless communications, that is, antennas, transceivers, and other electromagnetic wave transmitting equipment. BS's are typically fixed nodes, but they may also be used as part of mobile solutions, for example, a BS may be affixed to a vehicle to provide communications for near by Wi-max devices.

### Subscriber station (SS)

The SS is a stationary Wi-max capable radio system that communicates with a base station.

### Mobile station (MS)

An MS is an SS that is intended to be used while in motion at up to vehicular speeds. Compared with fixed (stationary) SS's, MS's typically are battery operated and therefore employ enhanced power management. Example MS's include Wi-max radios embedded in laptops and mobile phones.

### Relay station (RS)

RS's are SS's configured to forward traffic to other RS's or SS's in a multi-hop security zone. The RS may be in a

fixed location (e.g., attached to a building) or mobile (e.g., placed in an automobile).

## Operator network

The operator network encompasses infrastructure network functions that provide radio access and IP connectivity services to Wi-max subscribers. These functions are defined in Wi-max Forum technical specifications as the access service network (radio access) and the connectivity service network (IP connectivity). To make a communication, IEEE 802.16 used a four primary topologies networks that is, point-to-point, point-to-multipoint, multi-hop relay, and mobile. Now a day's popularity of internet protocol television (IPTV) is increasing because it gives us promise to deliver data to the user when it needed. IPTV provides service of video on demand (VOD) with video acquisition, video processed and video secure distribution which is received by user by using set up box (Jamil and Ravindra, 2013a; Wikipedia. Available at: <http://en.wikipedia.org/wiki/IPTV>; IPTV Focus Group. Available at: <http://www.itu.int/ITU/IPTV>). This service is provided to user with the help of Wi-max technology. There are many problems related to the transmission of video. This can be solved by using SVC codes. SVC is used because it provide better coding efficiency with an increased degree of supported scalability relative to the scalable profiles of prior video coding standards (Easwarakumar and Parvathi, 2012; Jamil and Ravindra, 2013b).

## RELATED WORK

Will and Ljiljana (2010) used the OPNET Modeller to engineer simulation sequences and explore the impact of channel bandwidth, time division duplex (TDD) frame size, advanced antenna systems support, and retransmission schemes movie to a Mobile Wi-max subscriber while streaming a feature-length. The performance was compared by using PLR, end-to-end (E2E) packet delays, and packet jitter matrices.

Thomas (2009), described brief overview of SVC when deployed in IPTV services is provided. It described the efficiency of various types of SVC analysis of the complexity of the various SVC tools. It also described how the different SVC features such as efficient methods for graceful degradation, bit rate adaptation and format adaptation, can be mapped to application requirements of IPTV services. It is discussed how such mappings can lead to improved content portability, management and distribution as well as an improved management of access network throughput resulting in better quality of service and experience for the users of IPTV services. There has no work to date on the effect of mobility on IPTV over Wi-max using SVC codes.

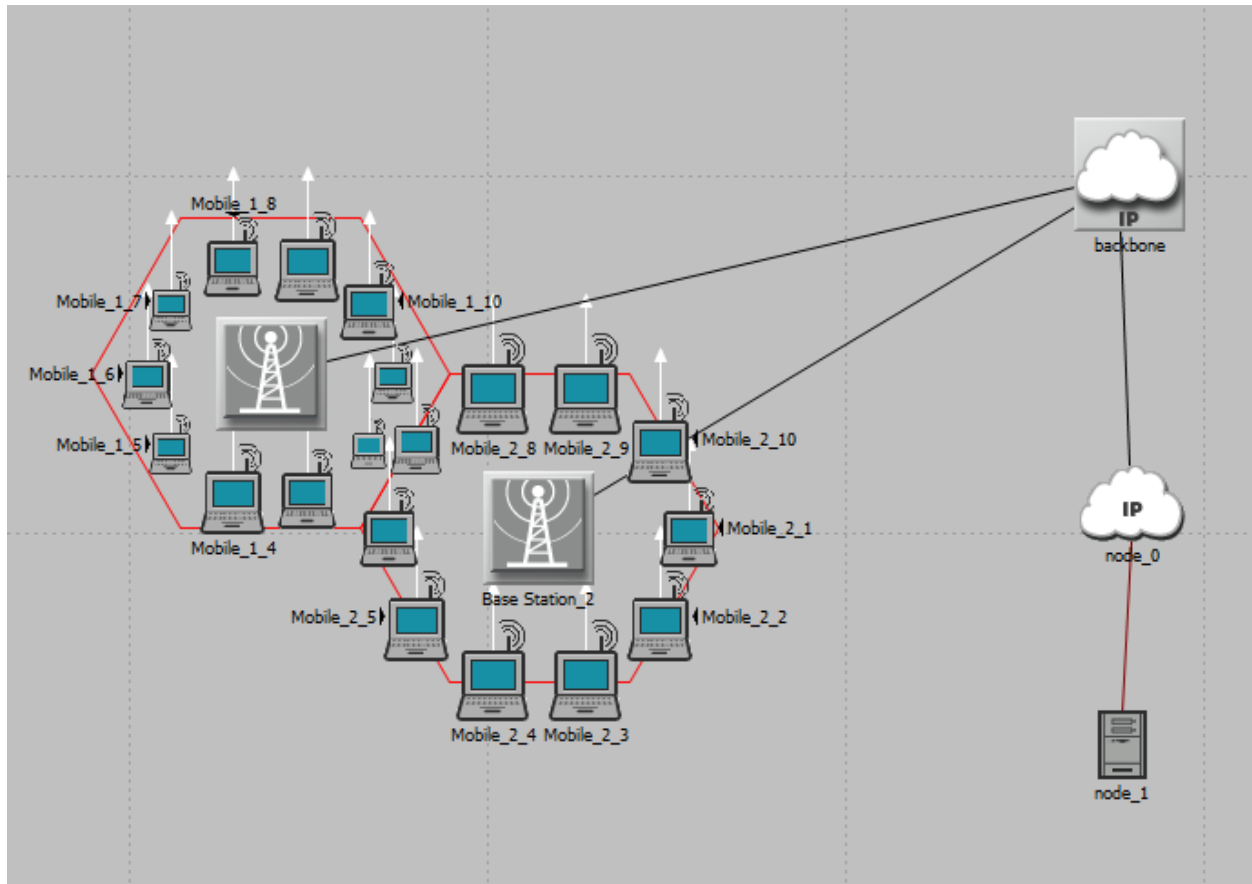


Figure 1. Model of Wi-max network.

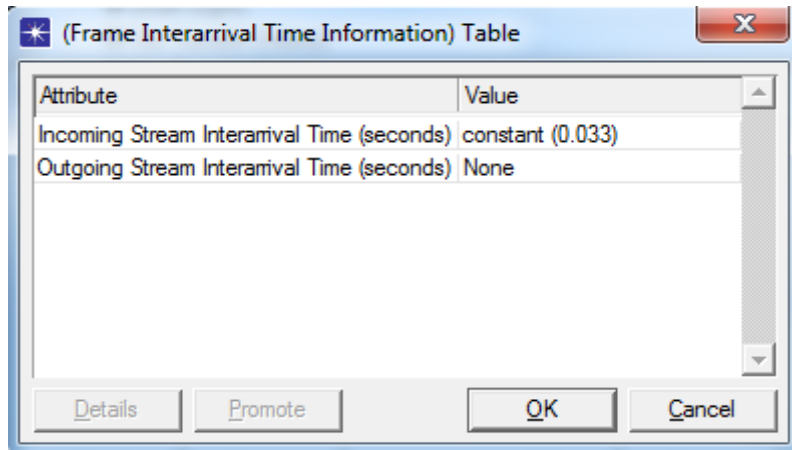
### Scalable video coding (SVC)

The SVC has been an active research and standardization area for at least 20 years. Prior international video coding standards such as H.262 MPEG-2Video H.263 and MPEG-4 visual already include several tools by which scalability can be supported. However, the scalable profiles of those standards have rarely been used. Reasons for that include the limitations of traditional video transmission systems as well as the fact that the spatial and quality scalability features came along with a significant loss in coding efficiency as well as a large increase in decoder complexity as compared to the corresponding non-scalable profiles. The recently standardized SVC extension of H.264/MPEG4-AVC (Schwarz et al., 2007) offers a significantly improved bit rate, distortion and complexity trade-off. But the deployment of a new video coding technology is also dependent on the business environment in which it is planned to be used. SVC offers a number of features that include efficient methods for graceful degradation, bit rate adaptation, and format adaptation. However, these features were not needed in traditional television broadcast via satellite, cable, or terrestrial channels.

In traditional broadcast, the transmission channel either works perfectly or is not working at all, making graceful degradation and (to some extent) also bit rate adaptation unnecessary. Moreover, the only deployed television format is standard definition; rendering format adaptation is not required. The recent introduction of television (TV) via IP-based access networks (IPTV) associated with heterogeneous terminal resolutions (PC, SD, HD-ready and Full-HD TV) creates the need for scalability.

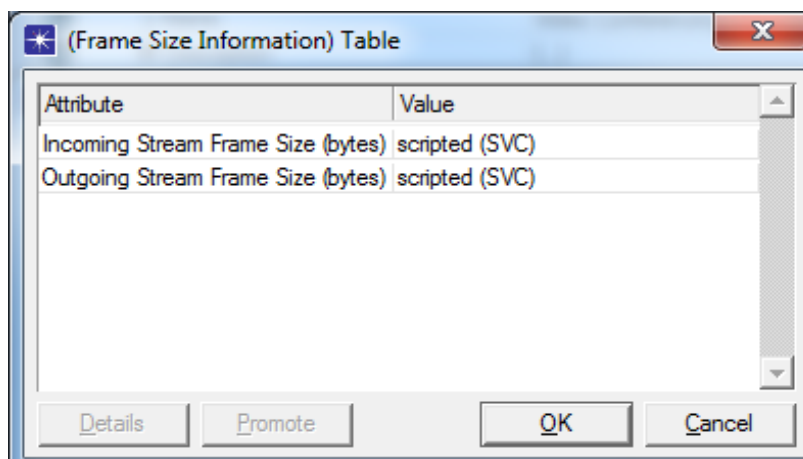
### EXPERIMENTAL SETUP

In this experiment the effect of mobility of mobile Wi-max subscriber on VOD over Wi-max is analyzed by using OPNET simulator. OPNET simulator 14.5 (OPNET official website, <http://www.opnet.com>) was used to analyse the performance of Wi-max. We used OPNET modeller, as OPNET modeller provides a comprehensive development environment supporting the modeling of communication network and distributed systems (Hammodi et al., 2009). OPNET modeller provides better environment for simulation, data collection and data analysis (OPNET official website, <http://www.opnet.com>). The basic model of this experiment is shown in Figure 1. In this experiment 4 scenarios with name Wi-max 6, Wi-max 7, Wi-max 8 and Wi-max 9 are taken. In these scenarios subscriber is moving with different mobility. In Wimax 6



Attribute	Value
Incoming Stream Interarrival Time (seconds)	constant (0.033)
Outgoing Stream Interarrival Time (seconds)	None

Figure 2. Frame inter-arrival time.



Attribute	Value
Incoming Stream Frame Size (bytes)	scripted (SVC)
Outgoing Stream Frame Size (bytes)	scripted (SVC)

Figure 3. Frame size.

subscriber have 60 km/h mobility, in Wimax 7 has 70 km/h, in Wimax 8 is 80 km/h and in Wimax 9 nodes have 90 km/h mobility. In each scenario two hexagonal cells are taken. Each cell has a radius of 2 Km, in each cell there is one base station and 10 mobile nodes. These nodes are circularly placed. The BS connected to the IP backbone via a DS3 WAN link. The node 0 is connected to backbone through ppp\_sonet\_oct1 link. The node 2 is also connected to video server through 100 base T Ethernet link.

#### Video application configuration

The frame inter-arrival time and the frame size parameters of the video conferencing application are shown in Figures 2 and 3. In this experiment the frame interval time was 30fps is taken for incoming and none for outgoing. The frame size for VOD is shown in Figure 3. In this experiment the SVC video codes are used which are shown in Table 1.

Figure 4 shows the profile configuration of VOD over Wi-max. In this experiment operation mode was simultaneous and start time was 1 s. The subscribers and video server is configured with this profile.

#### Wimax configuration

In Wi-max model RT PS scheduling class was created for the downlink and uplink to support the real time video streaming. The scheduling was configured with 5 Mbps, maximum sustainable traffic rate, and 1 Mbps minimum sustainable traffic rate as shown in Figure 5. The mobile Wi-max subscribers and base station is configured with match property of type of service (TOS). In each Wi-max subscribers the 64 QAM modulation and coding scheme is used for downlink and 16 QAM is used for uplink as shown in Figures 6 and 7. In this research, the matrix we measured is packet delay variation, packet end to end delay, delay and load.

#### RESULTS

Here the result of VOD over Wi-max is calculated by changing mobility of nodes. Figures 8 to 11 represents the result of packet delay variation, packet end to end delay, delay and load.

**Table 1.** Simulation parameter.

Parameter	SVC
Frame compression ratio	18.01
Min frame size (Bytes)	22
Max frame size (Bytes)	58150
Mean frame size (Bytes)	8440.74
Peak frame rate (Mbps)	13.9
Mean frame rates (Mbps)	2.02
Mean frame PSNR (dB)	47.89

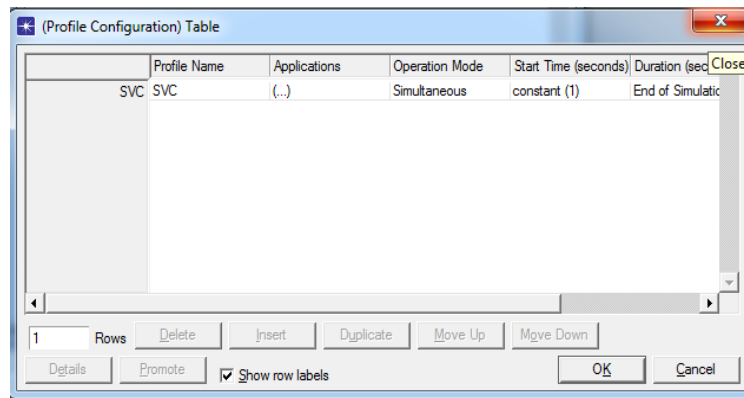


**Figure 4.** Profile configuration.

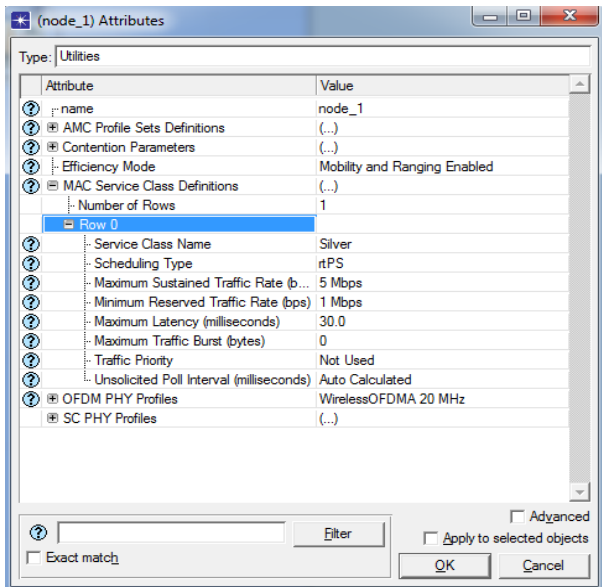


**Figure 5.** Classes configuration.

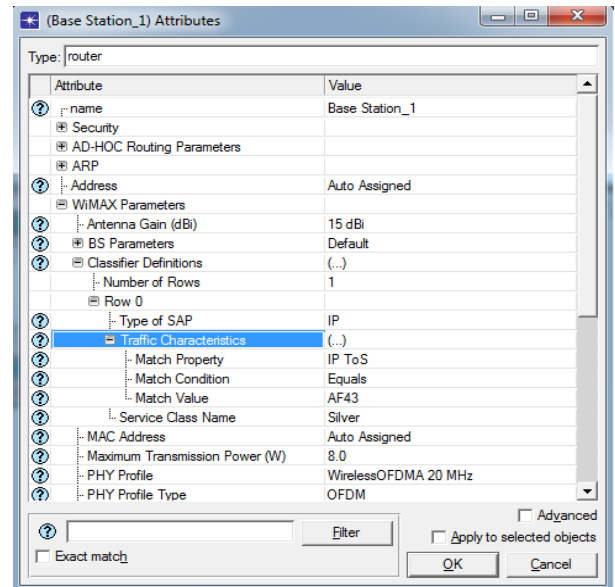


**Figure 6.** Base station parameters.

**Packet delay variations**

It is the variance among end to end delays for video

packets. End to end delay for a video packet is measured from the time it is created to the time it is received. Figure 8 shows the packet delay variation at different mobility.

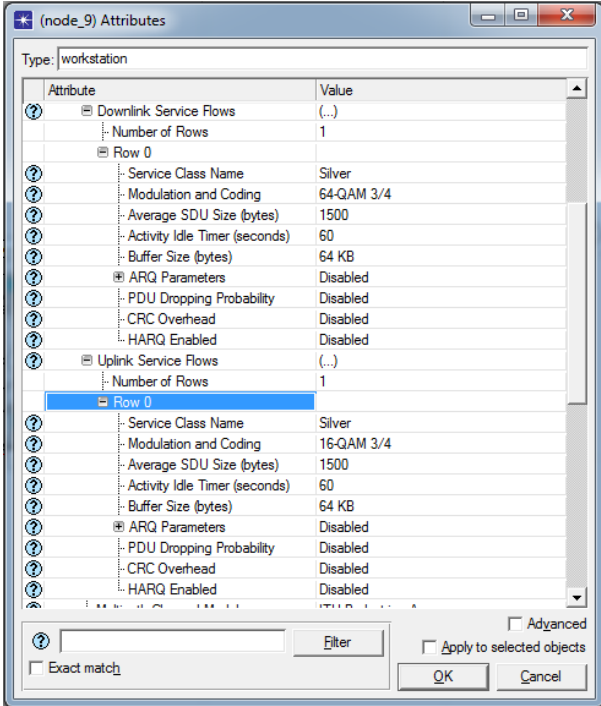


Figure 7. Wi-max subscriber station parameters.

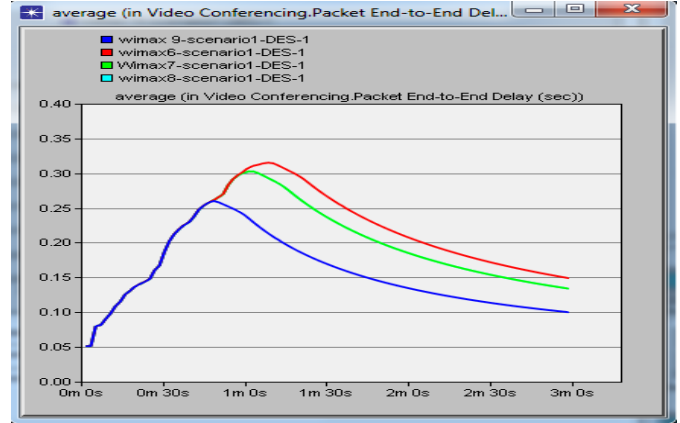


Figure 9. Packet end to end delay.

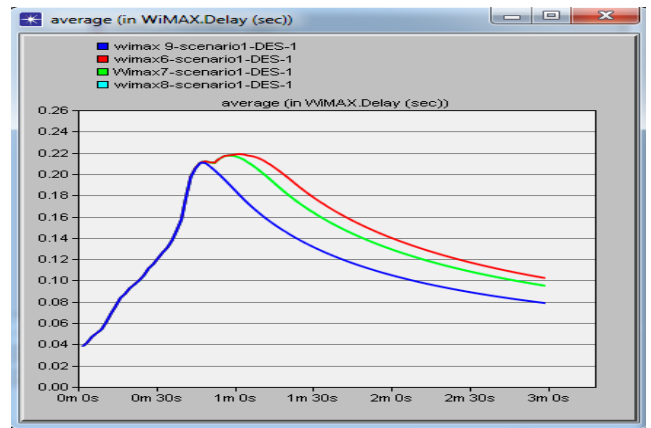


Figure 10. Delay.

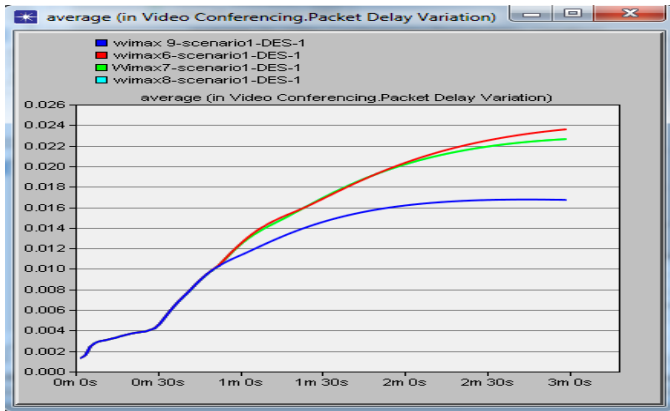


Figure 8. Packet delay variation.

Figure 8 shows that as the speed of the subscriber is increasing packet delay variation is decreasing. For 60 km/h the packet delay variation is 0.024 for 70 and 80 km/h it is 0.023 and for 90 km/h it is 0.017.

**Packet end to end delay**

It is the time taken to send a video application packet to a destination node application layer. This statistic records data from all the nodes in the network. Figure 9 shows that as speed is increasing, the packet end to end delay

is decreasing. From Figure 9, for 60 km/h, the highest value of packet end to end delay is 0.33 and for 70 and 80 km/h it is 0.30 and for 90 km/h it is 0.26.

**Delay**

It represents the end-to-end delay of all the packets received by the Wi-max MAC's of all Wi-max nodes in the network and forwarded to the higher layer. Figure 10 shows the result of Delay. Fig 10 shows that with increase in speed, the Delay decreases. Fig shows that at the end of simulation 60 km/hr have high delay which is 0.11, the delay for 70 km/hr and 80 km/hr is 0.09 and 90 km/hr has delay of 0.08.

**Load**

This represents the total load submitted to Wi-max layers by all higher layers in all Wi-max nodes of the network.

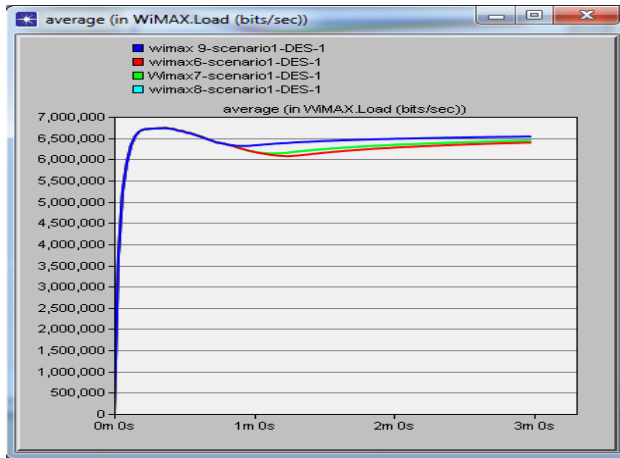


Figure 11. Load.

Figure 11 represents the result of Load. This figure shows that with increase in speed, the load also increases. From Figure 11, it has been observed that, 90 km/h having the highest load which is 6534877, 80 and 70 km/h having load of 6500000 and 60 km/h having load of 63916336.

## CONCLUSION AND FUTURE SCOPE

In this research, analysis of the performance of IPTV (VOD) over Wi-max by varying mobility of mobile Wi-max Subscriber in terms of packet delay variation, packet end to end delay, delay and load is carried out. In this experiment the placement of nodes are circular within hexagonal cell of radius 2 km. Here the speed of each node is varying from 60 to 90 km/h. For video streaming SVC codes are used. Simulation is carried out for three minutes. The results show that with increase in the speed, packet delay variation, packet end to end delay and delay are decreasing but the load is increasing, no doubt this increment of load is very little. The result also shows that for 70 and 80 km/h, the delay variation, packet end to end delay, delay and the load has equal values. In future, one can analyze the IPTV (VOD) over Wi-max by varying different parameters like network area, number of mobile Wi-max subscribers and power transmission.

## REFERENCES

- Aamir H, Christian MU, Markus R (2009). Performance Comparison Of Antenna Selection Algorithms In: Wi-max With Link Adaptation in Proc. 4th Int. Conf. Crowncom.
- Cicconetti C, Erta A, Lenzini L, Mingozzi E (2007). Performance evaluation of the IEEE 802.16 MAC for QOS support. In: IEEE Trans. mobile computing, 6:1.
- Daniel S (2004). Wi-max: operator's Manual Building 802.16 Wireless Networks. In: APRESS.
- Eklund C, Marks RB, Ponnuswamy S, Stanwood KL, Van NJM (2006). Wireless MAN, Inside the IEEE 802.16 Standard for Wireless Metropolitan Area Networks. IEEE Press.
- Schwarz H, Marpe D, Wiegand T (2007). Overview of the scalable video coding extension of the H.264/AVC standard In: IEEE Trans. Circuits Syst. Video Technol. Special Issue on Scalable Video Coding, 17(9):1103–1120.
- Hammoodi IS, Stewart BG, Kocian A, McMeekin SG (2009). A comprehensive performance Study of OPNET modeler for ZigBee WSN In: 3rd International conference on Next Generation Mobile Applications. pp. 357-362.
- IPTV Focus Group. Available at: <http://www.itu.int/ITU/IPTV>
- Jamil MH, Ravindra CT (2013a). INVESTIGATE THE PERFORMANCE EVALUATION OF IPTV OVER WIMAX NETWORKS In: (IJNCNC) 5:1.
- Jamil MH, Ravindra CT (2013b). Performance Evaluation of IPTV over Wi-max Networks Under Different Terrain Environments In: IJEEI. 2(2):21-25.
- Easwarakumar KS, Parvathi S (2012). Performance Evaluation of Multicast Video Streaming over Wi-max In: Int. J. Appl. Infor. Syst. 3:4.
- Mai T, George Z, Andrew N, Angela D (2008). Mobile Wi-max: Performance Analysis and Comparison with Experimental Results In: IEEE. pp. 1-5.
- OPNET official website, <http://www.opnet.com>.
- Rakesh KJ (2011). Security Analysis of Wi-max Network: With Misbehavior Node Attack in: IEEE. World Technol. WICT-2011, IEEE Xplore, pp. 397-404.
- Rakesh KJ, Suresh VL, Upena DD (2011). Performance Analysis under the Influence of Jamming for Wi-max System In: Second Int. Conf. Emerging Applications Info. Technol. 03/2011; DOI:10.1109/EAIT.2011.9.
- Saul R, Jad GA, Ana R (2010). A 2.3-ghz to 5.8-ghz cmos receiver front-end for wi-max/wlan In: IEEE.
- Shraddha B, Upadhyay R (2009). Performance of Different FEC Codes In First Int. Conf. Computational Intelligence, Commun. Syst. Networks. pp. 226-229.
- Thomas W (2009). Scalable Video Coding for IPTV Services in: IEEE 55:2.
- Wikipedia. Available at: <http://en.wikipedia.org/wiki/IPTV>.
- Will H, Ljiljana T (2010). Mobile Wi-max MAC and PHY layer optimization for IPTV In: Elsevier. Mathe. Comput. Modelling 53:2119–2135.

## **UPCOMING CONFERENCES**

**ICNMB 2013 : International Conference on Nuclear Medicine and  
Biology Switzerland, Zurich, July 30-31, 2013**



**International Conference on Mathematical Modeling in  
Physical Sciences Prague, Czech Republic, September 1-  
5, 2013**



## Conferences and Advert

### **July 2013**

ICNMB 2013 : International Conference on Nuclear Medicine and Biology  
Switzerland, Zurich, July 30-31, 2013

### **September 2013**

International Conference on Mathematical Modeling in Physical Sciences  
Prague, Czech Republic, September 1-5, 2013

# International Journal of Physical Sciences

## *Related Journals Published by Academic Journals*

- *African Journal of Pure and Applied Chemistry*
- *Journal of Internet and Information Systems*
- *Journal of Geology and Mining Research*
- *Journal of Oceanography and Marine Science*
- *Journal of Environmental Chemistry and Ecotoxicology*
- *Journal of Petroleum Technology and Alternative Fuels*

**academicJournals**